Higher-order predictions on diboson production within the MATRIX framework

Stefan Kallweit

Eur. Phys. J. Cxx (2018) no.xx, xxx [arXiv:1711.06631 [hep-ph]]
JHEP 1705 (2017) 139 [arXiv:1703.09065 [hep-ph]]
JHEP 1608 (2016) 140 [arXiv:1605.02716 [hep-ph]]
Phys. Lett. B761 (2016) 179-183 [arXiv:1604.08576 [hep-ph]]
Phys. Lett. B750 (2015) 407-410 [arXiv:1507.06257 [hep-ph]]
Phys. Rev. Lett. 113 (2014) 21, 212001 [arXiv:1408.5243 [hep-ph]]
Phys. Lett. B735 (2014) 311-313 [arXiv:1405.2219 [hep-ph]]

May 10, 2018, Joint Pheno Seminar @ Bicocca, Milan

Outline

1. Introduction
   - Motivation for NNLO QCD accuracy in VV production
2. Calculation of NNLO QCD cross sections in the MATRIX framework
   - Treatment of divergences by means of the q_{T} subtraction method
   - Implementation into the MUNICH Monte Carlo integrator
   - Technical studies on the q_{T}-cut dependence of cross sections
3. Numerical MATRIX results at NNLO QCD and data comparison
   - NNLO QCD results for $\mathrm{pp}\,(\to \mathrm{W}^{\pm}\mathrm{Z}) \to 3\ell\nu + \mathrm{X}$
   - NNLO QCD results for $\mathrm{pp}\,(\to \mathrm{W}^{+}\mathrm{W}^{-}) \to 2\ell 2\nu + \mathrm{X}$
   - NNLO QCD results for $\mathrm{pp}\,(\to \mathrm{ZZ}) \to 4\ell + \mathrm{X}$
4. Developments towards extensions of the MATRIX framework
   - Transverse-momentum resummation
   - NLO QCD corrections to loop-induced *gg* channel
   - NLO EW corrections
5. Conclusions

The MATRIX team

(Dirk Rathlev) Massimiliano Grazzini SK Marius Wiesemann

Importance of going beyond NLO in QCD for VV production

Fully exclusive NNLO QCD calculations desirable for several reasons

- Experimental accuracy has significantly increased – and will further increase.
- Usual variation of (unphysical) factorization and renormalization scales does not provide a reliable estimate of higher-order uncertainties at LO and NLO QCD.

  - All partonic channels are only included from NNLO on (only $q\bar{q}$ channels at LO).
  - Some phase-space regions are accessible only beyond LO (e.g. $p_{\mathrm{T,VV}} \neq 0$).
  - Jets are treated more realistically (VV+jet contribution only LO-accurate at NLO).

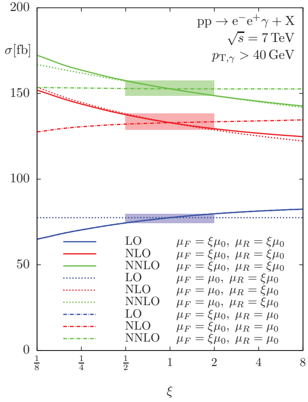

NLO EW corrections could contribute at the same order of magnitude, at least by naive counting of coupling constants, $\alpha_s^2 \approx \alpha$.

Leading N^{3}LO QCD corrections can be significant (namely the gg channel, which enters only at NNLO).

Data–theory comparison for VV cross sections — status spring 2014

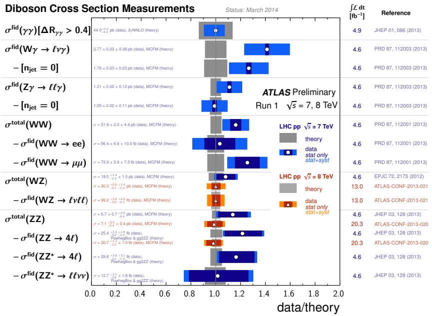

[ATLAS collaboration, March 2014]

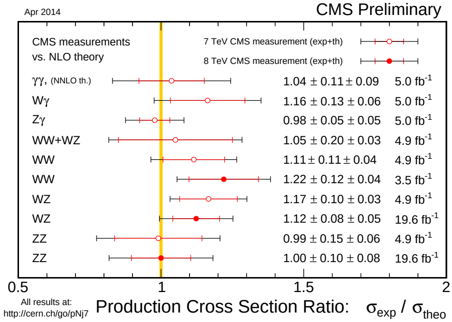

[CMS collaboration, April 2014]

Status of VV production about four years ago (after Run I)

- Only 7 TeV data and some (early) 8 TeV data analyzed by ATLAS and CMS.
- NLO QCD best available theory prediction for (almost) all processes.

↪ **Some moderate excesses ($\approx 2\sigma$) in experimental data,**
overall tendency to overshoot best available theory predictions (NLO QCD).

Data–theory comparison for VV cross sections — status summer 2017

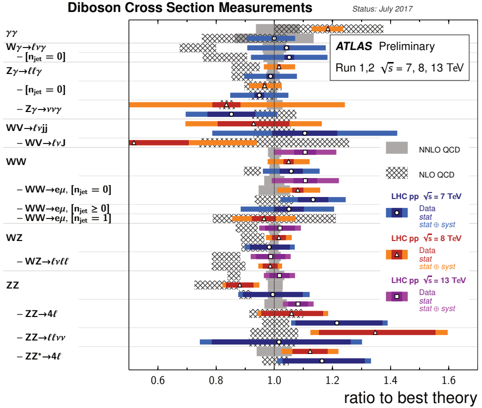

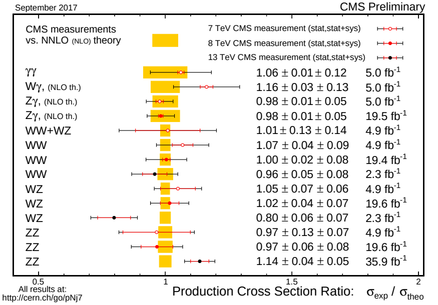

[CMS collaboration, September 2017]

[ATLAS collaboration, July 2017]

VV production (with leptonic decays) at NNLO QCD is important:

- Standard Model test → trilinear gauge-boson couplings
- Background for Higgs analyses and BSM searches

↪ **Inclusion of NNLO QCD corrections improves agreement with Standard Model.**

Calculation of NNLO QCD cross sections in the MATRIX framework

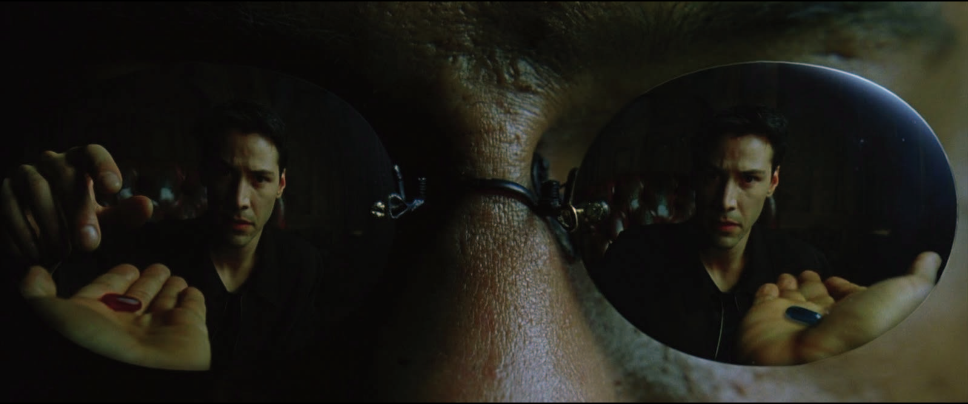

NLO QCD cross section via dipole subtraction

Schematic formula for the NLO cross section with dipoles [Catani, Seymour (1993)]

$$\delta\sigma^{\mathrm{NLO}} = \underbrace{\int_{m+1} d\sigma^R}_{\text{real}} + \underbrace{\int_m d\sigma^V}_{\text{virtual}} + \underbrace{\int_0^1 dz \int_m d\sigma^C}_{\text{collinear}} - \int_{m+1} d\sigma^A + \int_{m+1} d\sigma^A,$$

$$d\sigma^A = \sum_{\mathrm{dipoles}} d\sigma^B \otimes dV_{\mathrm{dipole}}$$

$$= \int_{m+1} \left[d\sigma^R - d\sigma^A \right]_{\epsilon=0} \qquad \Rightarrow \boldsymbol{\delta\sigma^{\mathrm{RA}}}$$

$$+ \int_m \left[d\sigma^V + \sum_{\mathrm{dipoles}} d\sigma^B \otimes V_{\mathrm{dipole}}(1) \right]_{\epsilon=0} \qquad \Rightarrow \boldsymbol{\delta\sigma^{\mathrm{VA}}}$$

$$+ \int_0^1 dz \int_m \left[d\sigma^C + \sum_{\mathrm{dipoles}} \int_1 d\sigma^B(z) \otimes [dV_{\mathrm{dipole}}(z)]_+ \right]_{\epsilon=0} \qquad \Rightarrow \boldsymbol{\delta\sigma^{\mathrm{CA}}}$$

$$dV_{\mathrm{dipole}}(z) = [dV_{\mathrm{dipole}}(z)]_+ + dV_{\mathrm{dipole}}(1)\delta(1-z)$$

↪ **Local subtraction terms** (Catani–Seymour dipole terms) allow for mediation of **infrared (soft and collinear) divergences** between the different phase spaces.

Idea of the q_T subtraction method for (N)NLO cross sections

Consider the production of a **colourless final state F** via $\mathbf{q\bar{q} \to F}$ or $\mathbf{gg \to F}$:

$$\mathrm{d}\sigma_{\mathrm{F}}^{\mathrm{(N)NLO}}\Big|_{q_T \neq 0} = \mathrm{d}\sigma_{\mathrm{F+jet}}^{\mathrm{(N)LO}},$$

where q_T refers to the transverse momentum of the colourless system F. [Catani, Grazzini (2007)]

$\mathrm{d}\sigma_{\mathrm{F}}^{\mathrm{(N)NLO}}\Big|_{q_T \neq 0}$ is singular for $q_T \to 0$, but the limiting behaviour is known from transverse-momentum resummation. [Bozzi, Catani, de Florian, Grazzini (2006)]

- Define a universal counterterm $\mathbf{\Sigma}$ with the complementary $q_T \to 0$ behaviour, $\mathrm{d}\sigma^{\mathrm{CT}} = \Sigma(q_T/Q) \otimes \mathrm{d}\sigma^{\mathrm{LO}}$, where Q is the invariant mass of the colourless system F.
- Add the $q_T = 0$ piece with the hard–virtual coefficient $\mathcal{H}_{\mathrm{F}}$, which is derived from the 1-(2-)loop amplitudes at (N)NLO, and also compensates for the subtraction of $\mathbf{\Sigma}$.

↪ **Full result for (N)NLO cross section**

$$\mathrm{d}\sigma_{\mathrm{F}}^{\mathrm{(N)NLO}} = \mathcal{H}_{\mathrm{F}}^{\mathrm{(N)NLO}} \otimes \mathrm{d}\sigma^{\mathrm{LO}} + \left[\mathrm{d}\sigma_{\mathrm{F+jet}}^{\mathrm{(N)LO}} - \Sigma^{\mathrm{(N)NLO}} \otimes \mathrm{d}\sigma^{\mathrm{LO}}\right]_{\mathrm{cut}_{q_T} \to 0}$$

Ingredients of the q_T subtraction method

$$d\sigma_{F}^{(N)NLO} = \mathcal{H}_{F}^{(N)NLO} \otimes d\sigma^{LO} + \left[d\sigma_{F+jet}^{(N)LO} - \Sigma^{(N)NLO} \otimes d\sigma^{LO} \right]_{cut_{q_T} \to 0}$$

- The hard–virtual coefficient $\mathcal{H}_F$,

$$\mathcal{H}_F = \underbrace{1}_{\text{tree-level amplitude}} + \underbrace{\left(\frac{\alpha_S}{\pi}\right) \mathcal{H}^{F(1)}}_{\text{contains (finite) 1-loop amplitude}} + \underbrace{\left(\frac{\alpha_S}{\pi}\right)^2 \mathcal{H}^{F(2)}}_{\text{contains (finite) 2-loop amplitude}} + \ldots,$$

  is known up to 2-loop order by means of a process-independent extraction procedure, starting from the all-order virtual amplitude of the specific process.
  [Catani, Cieri, de Florian, Ferrera, Grazzini (2013)]

- The counterterm $\Sigma(q_T/Q)$,

$$\Sigma(q_T/Q) = \left(\frac{\alpha_S}{\pi}\right) \Sigma^{(1)}(q_T/Q) + \left(\frac{\alpha_S}{\pi}\right)^2 \Sigma^{(2)}(q_T/Q) + \ldots,$$

  is universal (differs for $q\bar{q} \to F$ and $gg \to F$, trivial process dependence), and the coefficients are known (up to 2-loop order). [Bozzi, Catani, de Florian, Grazzini (2006)]

- The real-emission contribution $d\sigma_{F+jet}^{NLO}$ can be treated by any local NLO subtraction technique, e.g. by conventional dipole subtraction. [Catani, Seymour (1993)]

NLO QCD cross section via q_T subtraction

Schematic formula for the NLO cross section via q_T subtraction [Catani, Grazzini (2007)]

$$\delta\sigma^{\mathrm{NLO}} = \underbrace{\int_{m+1} d\sigma^R}_{\text{real}} + \underbrace{\int_m d\sigma^V}_{\text{virtual}} + \underbrace{\int_0^1 dz \int_m d\sigma^C}_{\text{collinear}}$$

$$= \int_{m+1} d\sigma^R \Big|_{q_T/q\,>\,\mathrm{cut}_{q_T/q}} \qquad \Rightarrow \text{finite, but depends on } \mathrm{cut}_{q_T/q}$$

$$+ \underbrace{\int_{m+1} d\sigma^R \Big|_{q_T/q\,\leq\,\mathrm{cut}_{q_T/q}}}_{\text{approximated by results known from } q_T \text{ resummation}} + \underbrace{\int_m d\sigma^V + \int_0^1 dz \int_m d\sigma^C}_{\text{identified with corresponding terms in } q_T \text{ resummation}}$$

$$\approx \int_{m+1} d\sigma^R \Big|_{q_T/q\,>\,\mathrm{cut}_{q_T/q}} + \frac{\alpha_S}{\pi} \boldsymbol{\mathcal{H}}^{\boldsymbol{F(1)}} \otimes \sigma_{\mathrm{LO}}$$

- no $\mathrm{cut}_{q_T/q}$ dependence,
- contains (finite) 1-loop part.

$$- \frac{\alpha_S}{\pi} \int_{\mathrm{cut}_{q_T/q}}^{\infty} d(q_T/q)\, \boldsymbol{\Sigma}^{(1)}(\boldsymbol{q_T/q}) \otimes \sigma_{\mathrm{LO}}$$

- cancels $\mathrm{cut}_{q_T/q}$ dependence,
- assigned to Born phase-space.

NNLO QCD cross section via q_T subtraction

Schematic formula for the NNLO cross section

$$\delta\sigma^{\mathrm{NNLO}} = \underbrace{\underbrace{\int_{m+2} d\sigma^{RR}}_{\text{double-real}} + \underbrace{\int_{m+1} d\sigma^{RV}}_{\text{real–virtual}} + \underbrace{\int_0^1 dz \int_{m+1} d\sigma^{RC}}_{\text{real–collinear}}}$$

$= \sigma^{\mathrm{NLO}}_{F+jet}$ $\Rightarrow$ at $q_\mathrm{T} \neq 0$ calculable via NLO subtraction, but divergent for $q_\mathrm{T} \to 0 \Rightarrow \mathrm{cut}_{q_\mathrm{T}/q}$

$$+ \underbrace{\int_m d\sigma^{VV}}_{\text{double-virtual}} + \underbrace{\int_0^1 dz \int_m d\sigma^{VC}}_{\text{virtual–collinear}} + \underbrace{\int_0^1 dz_1 \int_0^1 dz_2 \int_m d\sigma^{CC}}_{\text{double-collinear}}$$

$$= \sigma^{\mathrm{NLO}}_{F+jet}\Big|_{q_\mathrm{T}/q > \mathrm{cut}_{q_\mathrm{T}/q}}$$

$$+ \underbrace{\sigma^{\mathrm{NLO}}_{F+jet}\Big|_{q_\mathrm{T}/q \leq \mathrm{cut}_{q_\mathrm{T}/q}}}_{\substack{\text{approximated by results known}\\ \text{from } q_\mathrm{T} \text{ resummation}}} + \underbrace{\int_m d\sigma^{VV} + \int_0^1 dz \int_m d\sigma^{VC} + \int_0^1 dz_1 \int_0^1 dz_2 \int_m d\sigma^{CC}}_{\substack{\text{identified with corresponding terms}\\ \text{in } q_\mathrm{T} \text{ resummation}}}$$

NNLO QCD cross section via q_{T} subtraction

Schematic formula for the NNLO cross section

$$\delta\sigma^{\mathrm{NNLO}} = \underbrace{\left[\int_{m+2} d\sigma^{RRA} + \int_{m+1} d\sigma^{RVA} + \int_0^1 dz \int_{m+1} d\sigma^{RCA}\right]\Bigg|_{q_{\mathrm{T}}/q\,>\,\mathrm{cut}_{q_{\mathrm{T}}/q}}}_{=\,\sigma^{\mathrm{NLO}}_{F+jet}\big|_{q_{\mathrm{T}}/q\,>\,\mathrm{cut}_{q_{\mathrm{T}}/q}}}$$

$\Rightarrow$ finite, but depends on $\mathrm{cut}_{q_{\mathrm{T}}/q}$

$$-\left(\frac{\alpha_S}{\pi}\right)^2 \int_{\mathrm{cut}_{q_{\mathrm{T}}/q}}^{\infty} d(q_{\mathrm{T}}/q)\, \boldsymbol{\Sigma}^{(2)}(q_{\mathrm{T}}/q) \otimes \sigma_{\mathrm{LO}}$$

- cancels $\mathrm{cut}_{q_{\mathrm{T}}/q}$ dependence,
- contains (finite) 1-loop part,
- assigned to Born phase-space.

$$+\left(\frac{\alpha_S}{\pi}\right)^2 \boldsymbol{\mathcal{H}}^{F(2)} \otimes \sigma_{\mathrm{LO}}$$

- no $\mathrm{cut}_{q_{\mathrm{T}}/q}$ dependence,
- contains (finite) 2-loop part.

All relevant ingredients from q_{T} resummation ($\mathcal{H}^{F(i)}$, $\Sigma^{(i)}(q_{\mathrm{T}}/q)$ for $i \leq 2$) are known.

$\hookrightarrow$ **Direct implementation into a Monte Carlo integrator feasible.**

Numerical realization of the calculation

Realized within the fully automated NLO (QCD+EW) Monte Carlo framework
MUNICH (MUlti-chaNnel Integrator at Swiss (CH) precision) [SK]

- Applicable for arbitrary Standard Model processes (including partonic bookkeeping).
- Phase-space integration by highly efficient multi-channel Monte Carlo techniques
  ↪ Additional MC channels based on dipole kinematics constructed at runtime.
- OPENLOOPS interface, automatized implementation of dipole subtraction, etc.
- Simultaneous calculation for different scale choices and variations.

Extension to automated (q_T subtraction) NNLO QCD framework [Grazzini, SK, Rathlev]

- Process-independent construction of $\mathrm{cut}_{q_\mathrm{T}/q}$-dependent counterterms $\Sigma^{(1,2)}$.
- Process-independent extraction procedure for hard coefficients $\mathcal{H}^{(1,2)}$.
- Importance sampling performed on top of multi-channel approach
  ↪ improved efficiency and reliability in particular for low $\mathrm{cut}_{q_\mathrm{T}/q}$ values.
- Simultaneous evaluation of observables for different values of the regulator $\mathrm{cut}_{q_\mathrm{T}/q}$
  ↪ allows for monitoring of $\mathrm{cut}_{q_\mathrm{T}/q}$ and for extrapolation $\mathrm{cut}_{q_\mathrm{T}/q} \to 0$.

The MATRIX framework for automated NNLO+NNLL calculations

[Amplitude references → Backup]

[Grazzini, SK, Wiesemann (2017) + Rathlev,...]

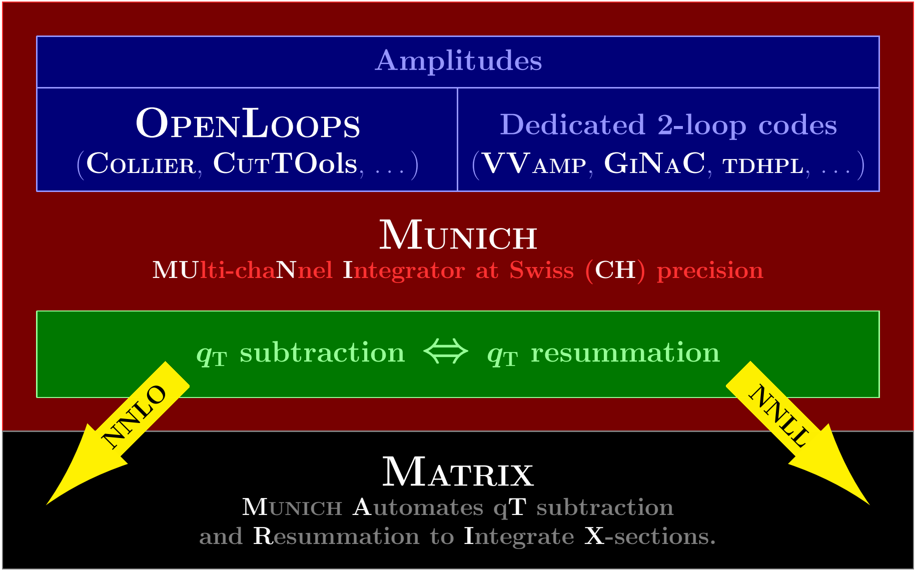

Processes available at NNLO QCD within the first MATRIX release

- **Single-boson production (essentially for validation)**
  - $\mathbf{pp \to Z/W^{\pm}\ (\to \ell\ell/\ell\nu) + X}$
    - agreement with ZWPROD (on-shell Z) [Hamberg, van Neerven, Matsuura (1991 & 2002)]
    - agreement with DYNNLO [Catani, Grazzini (2007); Catani, Cieri, Ferrera, de Florian, Grazzini (2009)]
    - agreement with NNLOJET [Gehrmann–De Ridder, Gehrmann, Glover, Huss, Morgan]
  - $\mathbf{pp \to H + X}$ $(m_t \to \infty)$
    - agreement with HNNLO [Catani, Grazzini (2007); Grazzini (2008); Grazzini, Sargsyan (2013)]
    - agreement with SUSHI [Harlander, Liebler, Mantler (2012)]
- **Boson-pair production (unknown before, apart from $\gamma\gamma$)**
  - $\mathbf{pp \to \gamma\gamma + X}$
    - agreement with 2GAMMANNLO [Catani, Cieri, Ferrera, de Florian, Grazzini (2011 & 2016 & 2018)]
    - agreement with MCFM [Campbell, Ellis, Li, Williams (2016)]
  - $\mathbf{pp \to Z\gamma/W^{\pm}\gamma\ (\to \ell\ell\gamma/\ell\nu\gamma/\nu\nu\gamma) + X}$
    - confirmation (Zγ) by MCFM [Campbell, Neumann, Williams (2017)]
  - $\mathbf{pp \to ZZ/W^+W^-/W^{\pm}Z\ (\to 4\ell/2\ell2\nu/3\ell\nu) + X}$ **(DF + SF channels)**
    - confirmation (on-shell ZZ) by [Heinrich, Jahn, Jones, Kerner, Pires (2017)]
  - $\mathbf{pp \to HH + X}$ $(m_t \to \infty)$ [de Florian, Grazzini, Hanga, SK, Lindert, Maierhöfer, Mazzitelli, Rathlev (2016)]
    (with m_t effects) [Grazzini, Heinrich, Jones, SK, Kerner, Lindert, Mazzitelli (2018)]
    - agreement with inclusive result $(m_t \to \infty)$ of [de Florian, Mazzitelli (2013 & 2015)]

  (performed in the MATRIX framework, but not provided in the first release)

Numerical stability and dependence on $\mathrm{cut}_{q_\mathrm{T}/q}$ in $\mathrm{pp} \to \gamma\gamma + X$

q_T subtraction at NLO

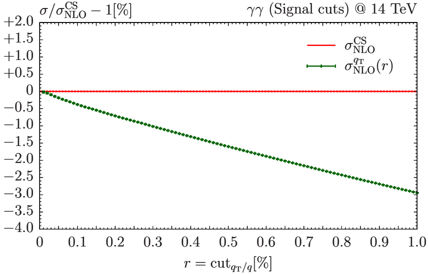

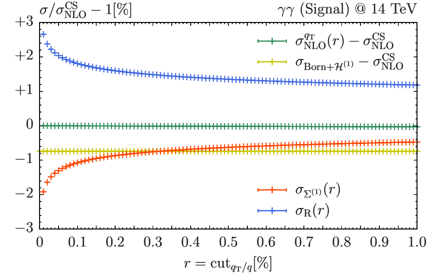

q_T subtraction at NNLO

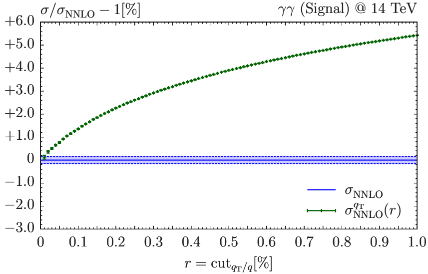

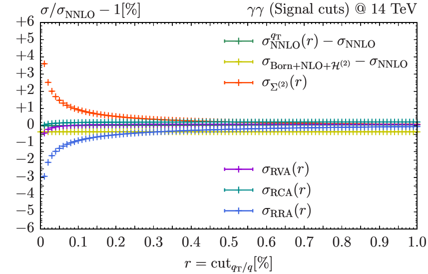

Numerical stability and dependence on $\mathrm{cut}_{q_T/q}$ in $\mathrm{pp} \to \mathrm{W}^\pm\mathrm{Z} + X$

q_T subtraction at NLO

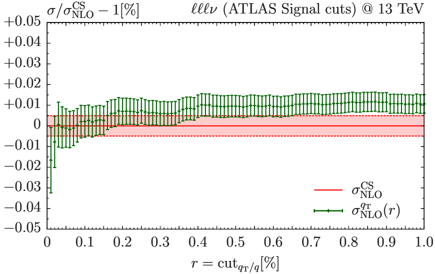

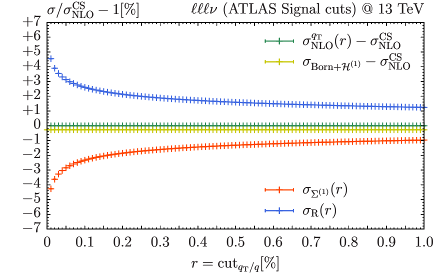

q_T subtraction at NNLO

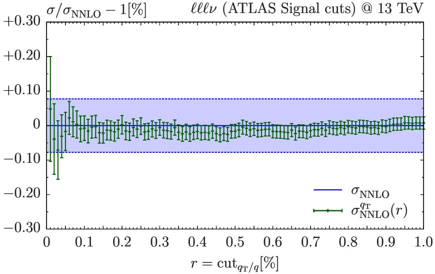

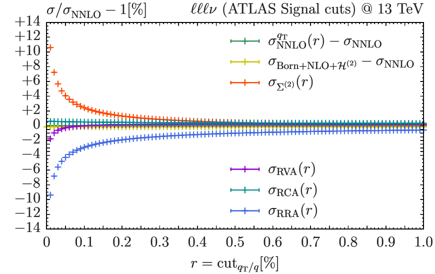

Automatic $r_{\mathrm{cut}} \to 0$ extrapolation in MATRIX – H/V production

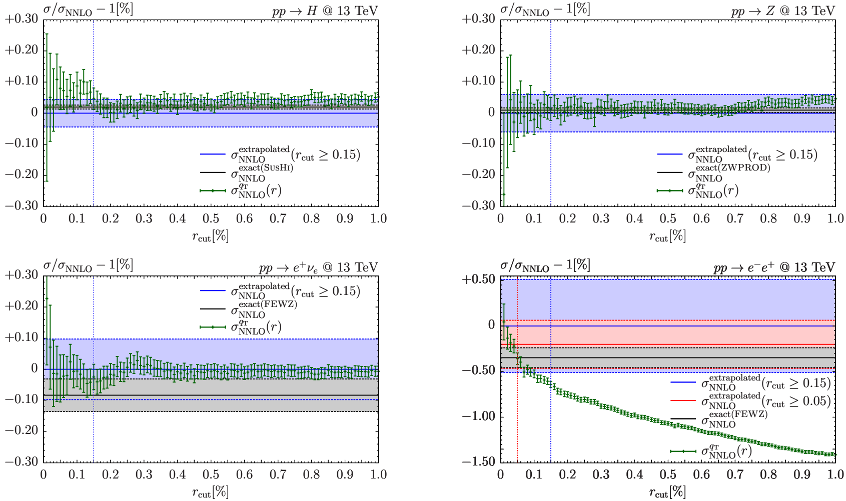

- **Simple quadratic fit** ($A \times r_{\mathrm{cut}}^2 + B \times r_{\mathrm{cut}} + C$) applied for $r_{\mathrm{cut}} \to 0$ extrapolation.
- **Error estimate** based on statistical error and variation of uppermost r_{cut} value.

Automatic $r_{\mathrm{cut}} \to 0$ extrapolation in MATRIX – VV production

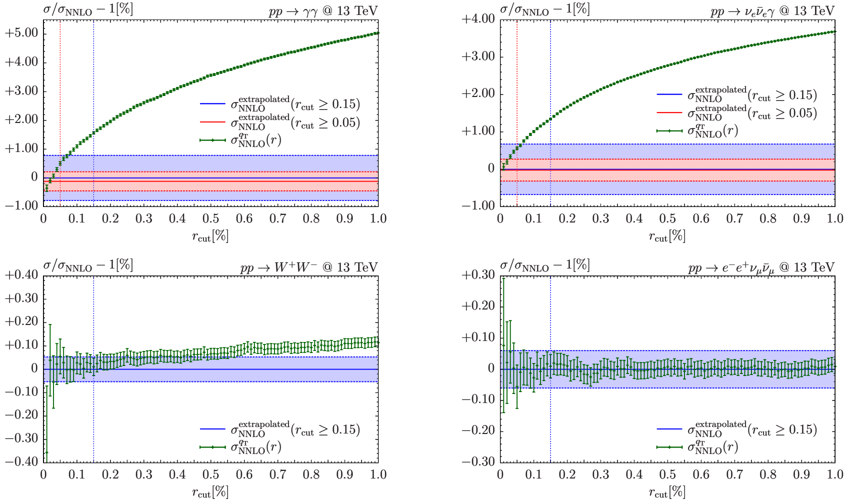

- **Simple quadratic fit** ($A \times r_{\mathrm{cut}}^2 + B \times r_{\mathrm{cut}} + C$) applied for $r_{\mathrm{cut}} \to 0$ extrapolation.
- **Error estimate** based on statistical error and variation of uppermost r_{cut} value.

Numerical MATRIX results at NNLO QCD and data comparison

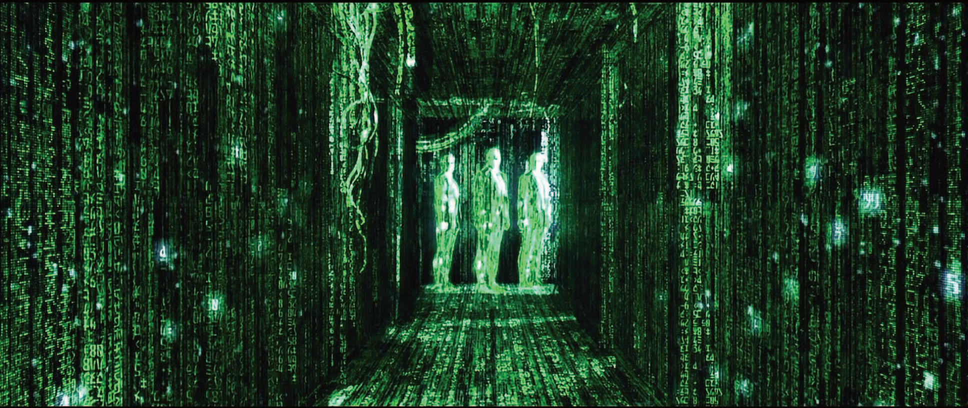

NNLO QCD results for $\mathrm{pp}\,(\to \mathrm{W}^{\pm}\mathrm{Z}) \to 3\ell\nu + \mathrm{X}$

[Grazzini, SK, Rathlev, Wiesemann (2016)]
[Grazzini, SK, Rathlev, Wiesemann (2017)]
[Grazzini, SK, Wiesemann (2017)]

$$\mathrm{pp} \to \mathrm{W}^{+}\ \mathrm{Z} + \mathrm{X}$$

$$\mathrm{pp} \to \mathrm{W}^{-}\ \mathrm{Z} + \mathrm{X}$$

$$\mathrm{pp}\ (\to \mathrm{W}^{+}\mathrm{Z}) \to \ell^{-}\ \ell^{+}\ \ell'^{+}\ \nu_{\ell'} + \mathrm{X}$$

$$\mathrm{pp}\ (\to \mathrm{W}^{-}\mathrm{Z}) \to \ell^{-}\ \ell'^{-}\ \ell^{+}\ \bar{\nu}_{\ell'} + \mathrm{X}$$

$$\mathrm{pp}\ (\to \mathrm{W}^{+}\mathrm{Z}) \to \ell^{-}\ \ell^{+}\ \ell^{+}\ \nu_{\ell} + \mathrm{X}$$

$$\mathrm{pp}\ (\to \mathrm{W}^{-}\mathrm{Z}) \to \ell^{-}\ \ell^{-}\ \ell^{+}\ \bar{\nu}_{\ell} + \mathrm{X}$$

Inclusive WZ cross sections for relevant LHC energies

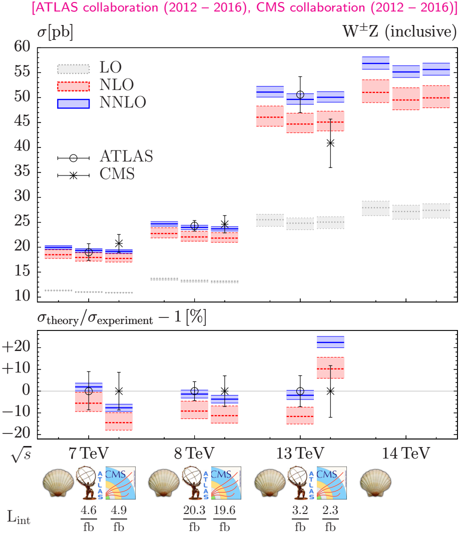

- MATRIX results with NNPDF3.0 PDF sets.

- **on-shell** (left): $m_{\ell\ell/\ell\nu} = m_{Z/W}$

  ATLAS (center):
  $66\,\text{GeV} < m_{\ell\ell} < 116\,\text{GeV}$

  CMS (right):
  $71\,\text{GeV} < m_{\ell\ell} < 111\,\text{GeV}$
  (7 TeV and 8 TeV)
  $60\,\text{GeV} < m_{\ell\ell} < 120\,\text{GeV}$
  (13 TeV and 14 TeV)

- NLO/LO ranges from 63% to 83% (7 TeV to 14 TeV) (approximate radiation zero).

- NNLO/NLO ranges from 8% to 11% (7 TeV to 14 TeV).

- NNLO scale variation ≈ ±2% with $\mu_0 = (M_W + M_Z)/2$.
  $$\begin{pmatrix} \mu_0/2 \le \mu_R, \mu_F \le 2\mu_0 \\ 1/2 \le \mu_R/\mu_F \le 2 \end{pmatrix}$$

- No NLO EW included.

Distributions for $\mathrm{pp}\,(\to \mathrm{W}^{\pm}\mathrm{Z}) \to 3\ell\nu + \mathrm{X}$ at NNLO QCD

data points taken from [ATLAS collaboration, PHYSICAL REVIEW D 93, 092004 (2016)]

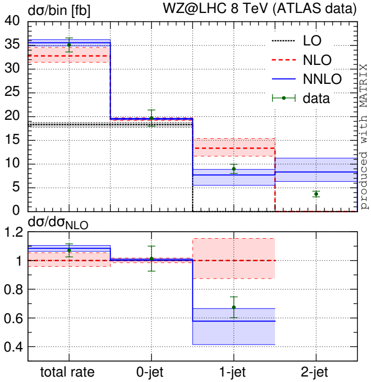

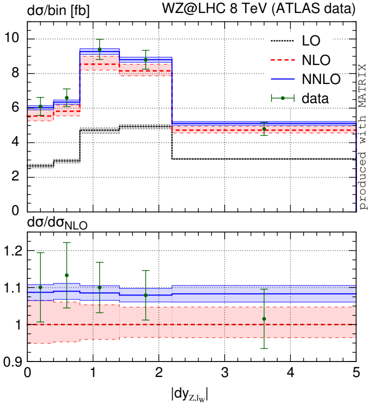

- **Jet-multipliciy distribution (left)**: Very small NNLO corrections in 0-jet bin.

  Note: Only 0-jet bin is NNLO-accurate; 1(2)-jet bin is only NLO(LO)-accurate.
- $|\mathrm{d}y_{\mathrm{Z},\mathrm{l_W}}|$ **distribution (right)**: Approximate radiation zero leads to dip around 0.

  ↪ Improved agreement at NNLO solely due to normalization correction.

Distributions for $pp\,(\rightarrow W^{\pm}Z) \rightarrow 3\ell\nu + X$ at NNLO QCD

data points taken from [ATLAS collaboration, PHYSICAL REVIEW D 93, 092004 (2016)]

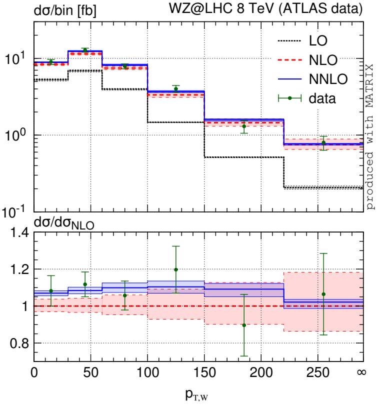

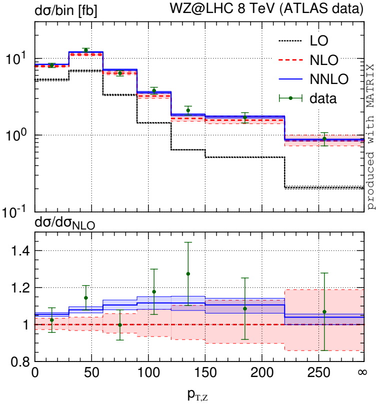

- **Distribution in vector-boson transverse momenta: $p_{T,W}$ (left) and $p_{T,Z}$ (right):** (vector bosons reconstructed via "resonant shape" algorithm in SF channel)
  - NNLO corrections in normalization and shape improve agreement with data.
  - Scale dependence is significantly reduced at NNLO also on a differential level.

Distributions for $\mathrm{pp}\,(\to \mathrm{W}^{\pm}\mathrm{Z}) \to 3\ell\nu + \mathrm{X}$ at NNLO QCD

data points taken from [ATLAS collaboration, PHYSICAL REVIEW D 93, 092004 (2016)]

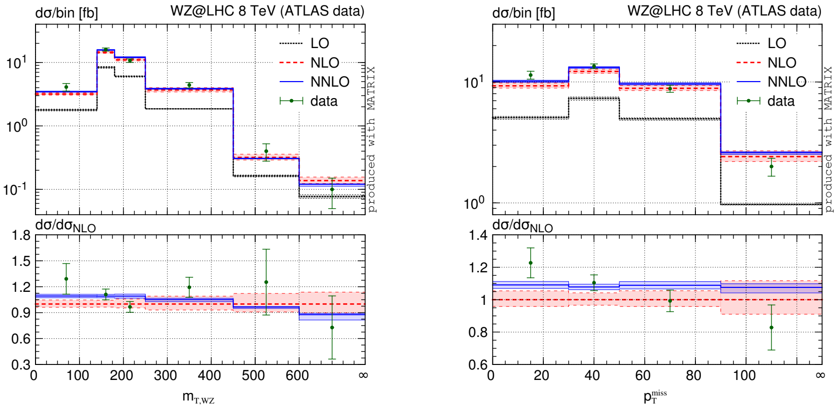

- **Distribution in transverse WZ mass (left)**: $m_{T,WZ} = \left(\sum E_{T,\ell} + E_{T,\nu}\right)^2 - p^2_{\mathrm{T},\ell\ell\ell\nu}$
  - ↪ Shape effects of about 15% at NNLO slightly improve the agreement.
- **Distribution in missing transverse momentum (right)**:
  - ↪ Some tension between data and NNLO prediction, but only in $\mathrm{W}^{-}\mathrm{Z}$ process.

NNLO QCD results for $\mathrm{pp}\,(\to \mathrm{W^+W^-}) \to 2\ell 2\nu + \mathrm{X}$

[Gehrmann, Grazzini, SK, Maierhöfer, von Manteuffel, Pozzorini, Rathlev, Tancredi (2014)]
[Grazzini, SK, Pozzorini, Rathlev, Wiesemann (2016)]
[Grazzini, SK, Wiesemann (2017)]

$$\mathrm{pp} \to \mathrm{W^+} \; \mathrm{W^-} + \mathrm{X}$$

$$\mathrm{pp} \; (\to \mathrm{W^+W^-}) \to \ell^- \; \ell'^+ \; \nu_{\ell'} \; \bar{\nu}_\ell + \mathrm{X}$$

$$\mathrm{pp} \; (\to \mathrm{W^+W^-/ZZ}) \to \ell^- \; \ell^+ \; \nu_\ell \; \bar{\nu}_\ell + \mathrm{X}$$

Inclusive WW cross sections for relevant LHC energies

[ATLAS collaboration (2012 – 2017), CMS collaboration (2012 – 2016)]

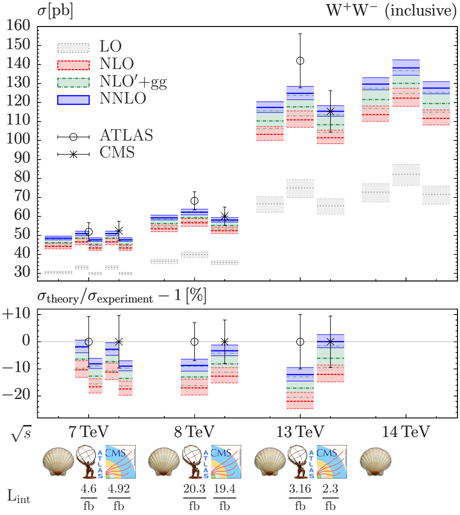

- **MATRIX** results with NNPDF3.0 PDF sets.

- **on-shell** (left): $m_{\ell\nu} = m_W$
  ATLAS (center): 8, 13, 14 TeV: $H \to WW^*$ included
  CMS (right): 8, 13, 14 TeV: $H \to WW^*$ not included
  ATLAS and **CMS**: 7 TeV: Predictions shown with (left) and without (right) $H \to WW^*$

- NLO/LO ranges from 44% to 56% (7 TeV to 14 TeV).

- NNLO/NLO ranges from 10% to 14% (7 TeV to 14 TeV).

- Loop-induced gg channel makes for about 35% of NNLO effect.

- NNLO scale variation $\approx \pm 3\%$.

$$\begin{pmatrix} M_W/2 \le \mu_R, \mu_F \le 2M_W \\ 1/2 \le \mu_R/\mu_F \le 2 \end{pmatrix}$$

Corrections to WW production beyond NNLO QCD

NLO QCD corrections to gg $\to \mathrm{W^+W^-}$ (gg-channel, massless 2-loop amplitudes)
[Caola, Melnikov, Röntsch, Tancredi (2015)]
(based on amplitudes from [Caola, Henn, Melnikov, Smirnov, Smirnov (2015); von Manteuffel, Tancredi (2015)])

- The LO gg-fusion cross section is increased by $\mathcal{O}(24\% - 80\%)$ for $M_\mathrm{W}/2 < \mu_\mathrm{R} = \mu_\mathrm{F} < 2M_\mathrm{W}$ at $\sqrt{s} = 8\,\mathrm{TeV}$ (slightly smaller at $\sqrt{s} = 13\,\mathrm{TeV}$).
  - ↪ Corresponds to increase of full NLO QCD prediction by about **+2%** at $\sqrt{s} = 8$ and $13\,\mathrm{TeV}$ (covered by the NNLO QCD scale-uncertainty estimate).
- In the ATLAS fiducial region, NLO QCD corrections to gg shrink to about $+20\%$.
- **NLO QCD to gg $\to \mathrm{W^+W^-}$** including interference effects with off-shell Higgs.
  [Caola, Dowling, Melnikov, Röntsch, Tancredi (2016)]

NLO EW corrections to off-shell $\mathrm{W^+W^-}$ production
[Biedermann, Billoni, Denner, Dittmaier, Hofer, Jäger, Salfelder (2016)], [SK, Lindert, Pozzorini, Schönherr (2017)]

- Corrections of about **−4% (−3%)** wrt. the inclusive (fiducial ATLAS) cross section at LO for both $\sqrt{s} = 8$ and $13\,\mathrm{TeV}$.
  - ↪ Larger (typically tens of per cent) corrections at high transverse momenta.
- Contribution from **$\gamma\gamma$-induced process** of about **+1%** wrt. both the inclusive and the fiducial ATLAS cross section at LO for both $\sqrt{s} = 8$ and $13\,\mathrm{TeV}$.

Definition of top-contamination free WW cross section

- Straightforward in 4FNS (massive b's $\to$ $\mathrm{WWb\bar{b}}$ finite and can be split off)
- Non-trivial in 5FNS (massless b's $\to$ WW and $\mathrm{WWb\bar{b}}$ connected by IR structure)
  - Single-top production enters at NLO.
  - Top-pair production enters at NNLO.

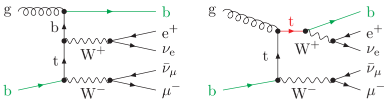

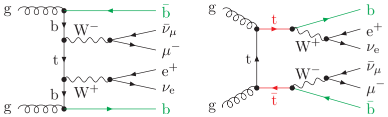

↪ Huge "higher-order corrections" result from top-resonance contamination in 5FNS (cross-section enhancement of 30%/400% at NLO/NNLO for $\sqrt{s} = 8$ TeV).

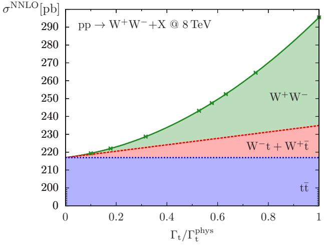

- Γ_t-dependence of NNLO cross section can be used to isolate the different processes:

  $\sigma_{\mathrm{WW}} \propto 1, \quad \sigma_{\mathrm{tW}} \propto 1/\Gamma_t, \quad \sigma_{t\bar{t}} \propto 1/\Gamma_t^2.$

- Parabolic fit of $(\Gamma_t/\Gamma_t^{\mathrm{phys}})^2$-rescaled NNLO cross section delivers σ_{WW}, σ_{tW}, $\sigma_{t\bar{t}}$.

↪ $\approx$ 1-2% agreement between 4FNS and 5FNS.

Fiducial off-shell cross sections for $\mathrm{pp}\,(\rightarrow \mathrm{W}^+\mathrm{W}^-) \rightarrow 2\ell 2\nu + \mathrm{X}$

Setup motivated by the ATLAS analysis @ 8 TeV [ATLAS collaboration (2014 & 2016)]

	$\sigma_{\text{fiducial}}(W^+W^-\text{-cuts})$ [fb]		$\sigma/\sigma_{\text{NLO}} - 1$	
$\sqrt{s}$	8 TeV	13 TeV	8 TeV	13 TeV
LO	$147.23\ (2)\ ^{+3.4\%}_{-4.4\%}$	$233.04(2)\ ^{+6.6\%}_{-7.6\%}$	-3.8%	$-\ 1.3\%$
NLO	$153.07\ (2)\ ^{+1.9\%}_{-1.6\%}$	$236.19(2)\ ^{+2.8\%}_{-2.4\%}$	0	0
NLO′	$156.71\ (3)\ ^{+1.8\%}_{-1.4\%}$	$243.82(4)\ ^{+2.6\%}_{-2.2\%}$	$+2.4\%$	$+\ 3.2\%$
NLO′+gg	$166.41\ (3)\ ^{+1.3\%}_{-1.3\%}$	$267.31(4)\ ^{+1.5\%}_{-2.1\%}$	$+8.7\%$	$+13.2\%$
NNLO	$164.16(13)\ ^{+1.3\%}_{-0.8\%}$	$261.5(2)\ ^{+1.9\%}_{-1.2\%}$	$+7.2\%$	$+10.7\%$

- Results refer to only one different-flavour channel: $\boldsymbol{pp \rightarrow \mathrm{e}^-\mu^+\nu_\mu\bar{\nu}_\mathrm{e} + \mathrm{X}}$
- Event selection imposes a **jet veto**.
  - ↪ Usual scale variation underestimates missing higher-order corrections.
- NLO corrections amount to about $+4\%$ $(+1\%)$ wrt. LO result at 8 (13) TeV.
- NNLO corrections amount to about $+7\%$ $(+10\%)$ wrt. NLO result at 8 (13) TeV.
- The positive impact of the NNLO corrections is entirely due to the loop-induced gg contribution, which is about $+6\%$ $(+10\%)$ wrt. NLO result at 8 (13) TeV.
  - ↪ $\mathcal{O}(\alpha_\mathrm{s}^2)$ corrections to $q\bar{q}$ are negative and amount to roughly -2% (-3%).

Distributions for $pp(\to WW) \to 2\ell 2\nu + X$ at NNLO QCD

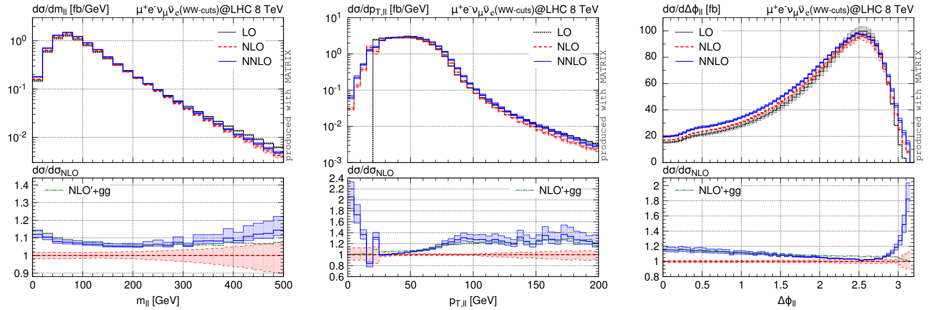

- NLO and NNLO scale-variation bands typically do not overlap.
  - ↪ The loop-induced *gg* contribution dominates the NNLO corrections.
- By and large the $\text{NLO}' + gg$ approximates the full NNLO prediction very well.
- However, shape distortions of up to 10% result from genuine NNLO corrections.
- In phase-space regions that imply the presence of QCD radiation, the loop-induced gg contribution cannot approximate the shapes of full NNLO corrections.

NNLO QCD results for $\mathrm{pp}\,(\to \mathrm{ZZ}) \to 4\ell + \mathrm{X}$

[Cascioli, Gehrmann, Grazzini, SK, Maierhöfer, von Manteuffel, Pozzorini, Rathlev, Tancredi, Weihs (2014)]
[Grazzini, SK, Rathlev (2015)]
[Grazzini, SK, Wiesemann (2017)]

$$\mathrm{pp} \to \mathrm{Z}\ \mathrm{Z} + \mathrm{X}$$

$$\mathrm{pp}\ (\to \mathrm{ZZ}) \to \ell^- \ \ell^+ \ \ell'^- \ \ell'^+ + \mathrm{X}$$

$$\mathrm{pp}\ (\to \mathrm{ZZ}) \to \ell^- \ \ell^+ \ \ell^- \ \ell^+ + \mathrm{X}$$

$$\mathrm{pp}\ (\to \mathrm{ZZ}) \to \ell^- \ \ell^+ \ \nu_{\ell'} \ \bar{\nu}_{\ell'} + \mathrm{X}$$

$$\mathrm{pp}\ (\to \mathrm{W^+W^-/ZZ}) \to \ell^- \ \ell^+ \ \nu_{\ell} \ \bar{\nu}_{\ell} + \mathrm{X}$$

Inclusive ZZ cross sections for relevant LHC energies

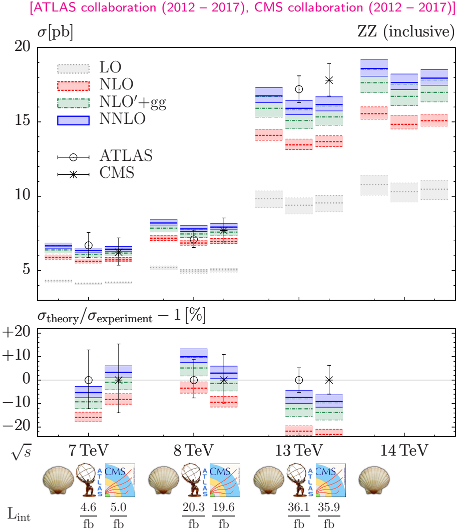

- **MATRIX** results with NNPDF3.0 PDF sets.

- **on-shell** (left): $m_{\ell\ell} = m_Z$
  ATLAS (center):
  $66\,\mathrm{GeV} < m_{\ell\ell} < 116\,\mathrm{GeV}$
  CMS (right):
  $60\,\mathrm{GeV} < m_{\ell\ell} < 120\,\mathrm{GeV}$

- NLO/LO ranges from 36% to 44% (7 TeV to 14 TeV).
- NNLO/NLO ranges from 12% to 17% (7 TeV to 14 TeV).
- Loop-induced gg channel makes for about 60% of NNLO effect.
- NNLO scale variation ≈ ±3%.
  $$\begin{pmatrix} M_Z/2 \le \mu_R, \mu_F \le 2M_Z \\ 1/2 \le \mu_R/\mu_F \le 2 \end{pmatrix}$$
- No NLO EW or NLO QCD to gg-fusion channel included.

Corrections to ZZ production beyond NNLO QCD

NLO QCD corrections to gg → ZZ (gg-channel, massless 2-loop amplitudes)
[Caola, Melnikov, Röntsch, Tancredi (2015)]
(based on amplitudes from [Caola, Henn, Melnikov, Smirnov, Smirnov (2015); von Manteuffel, Tancredi (2015)])

- The LO gg-fusion cross section is increased by $\mathcal{O}(60\% - 110\%)$ for $M_\mathrm{Z} < \mu_\mathrm{R} = \mu_\mathrm{F} < 4M_\mathrm{Z}$ at $\sqrt{s} = 8\,\mathrm{TeV}$ (slightly smaller at $\sqrt{s} = 13\,\mathrm{TeV}$).

↪ Corresponds to increase of full NLO QCD prediction by about **+6%** at $\sqrt{s} = 8\,\mathrm{TeV}$ and $13\,\mathrm{TeV}$ (correction exceeds the NNLO QCD scale band).

- **NLO QCD to gg → ZZ** including interference effects with off-shell Higgs.
  [Caola, Dowling, Melnikov, Röntsch, Tancredi (2016)]
- **NLO QCD to gg → ZZ** matched to parton shower in POHWEG.
  [Alioli, Caola, Luisoni, Röntsch (2016)]

NLO EW corrections to off-shell ZZ production
[Biedermann, Denner, Dittmaier, Hofer, Jäger (2016 & 2016)]

- Corrections of about **−4%** to the inclusive (LO) cross section at $\sqrt{s} = 8\,\mathrm{TeV}$.
  ↪ Larger (typically tens of per cent) corrections at high transverse momenta.

↪ **Both corrections are quantitatively relevant,** also at the level of inclusive cross sections, but happen to partially cancel.

Recent experimental results for $\mathrm{pp}\,(\to \mathrm{ZZ}) \to 4\ell + \mathrm{X}$ at 13 TeV

Inclusive *ZZ* cross sections

[ATLAS collaboration (2017)]

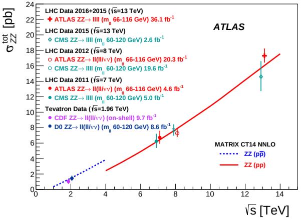

[CMS collaboration (2017)]

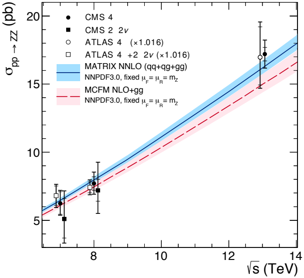

Fiducial 4ℓ cross sections

[ATLAS collaboration (2017)]

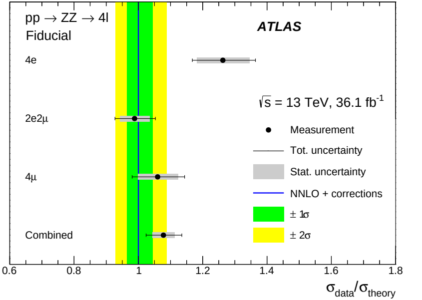

"NNLO + corrections" is defined as

- fully differential NNLO QCD from MATRIX
  [Grazzini, SK, Wiesemann (2017)]
- LO *gg* channel reweighted by global *K*-factor
  [Caola, Melnikov, Röntsch, Tancredi (2015)]
- EW *K*-factor applied (bin-wise, where applicable)
  [Biedermann, Denner, Dittmaier, Hofer, Jäger (2016 & 2016)]
- EW-ZZjj channel added at its LO $\mathcal{O}(\alpha^6)$

Recent ATLAS results for $\mathrm{pp}\,(\to \mathrm{ZZ}) \to 4\ell + \mathrm{X}$ at 13 TeV

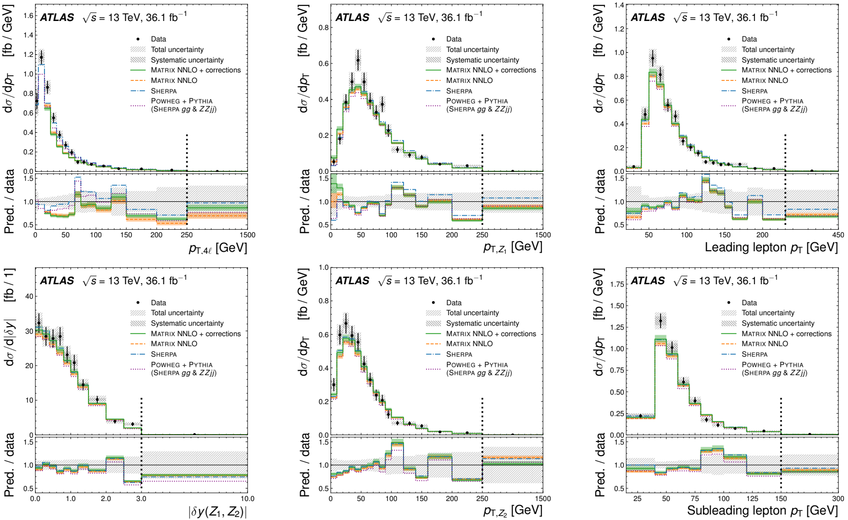

[ATLAS collaboration (2017)]

- Comparison to **MATRIX** results (+ corrections: **NLO EW**, **NLO QCD to *gg***, **VBF**)

  ↪ Reasonable agreement within (statitistics-dominated) experimental errors.

Developments towards extensions of the MATRIX framework

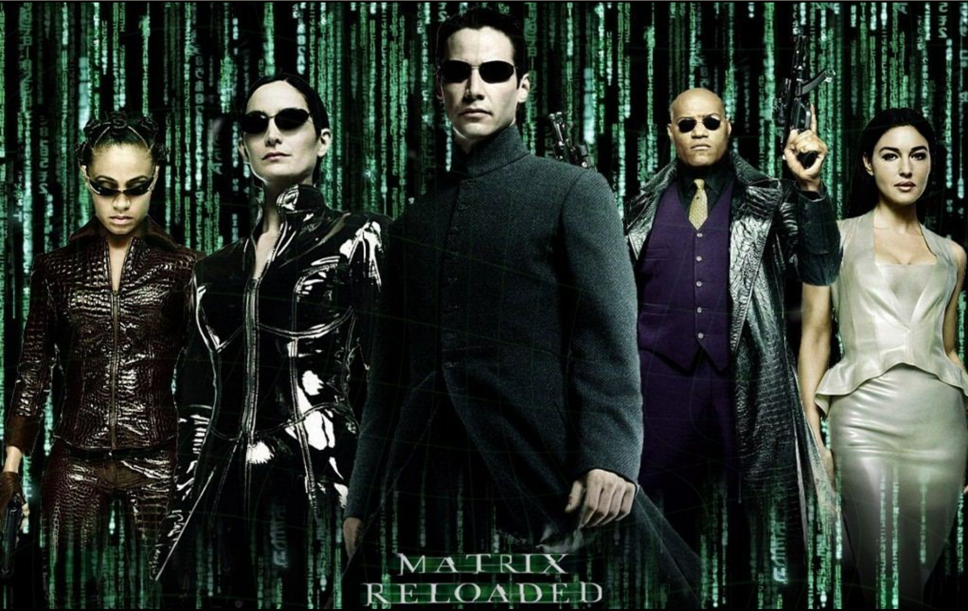

Transverse-momentum resummation at NNLL + NNLO QCD

- **Production of colourless system $\mathcal{F}$** (invariant mass M, p_{T})
- Problem: p_{T} distribution of $\mathcal{F}$ diverges for $p_{\mathrm{T}} \to 0$ at fixed order
- Reason: Large logarithms $\log(p_{\mathrm{T}}^2/M^2)$ for $p_{\mathrm{T}} \ll M$
- Solution: All-order resummation of logarithms

[Grazzini, SK, Rathlev, Wiesemann (2015)]

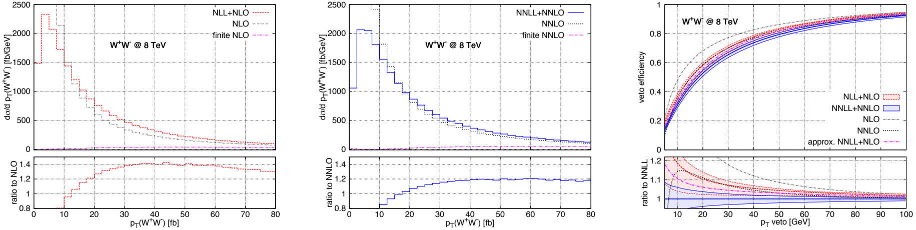

Status of transverse-momentum resummation within the MATRIX framework:

- First application on WW/ZZ production, leptonic final states under validation
- Implementation for charged system $\mathcal{F}$ (i.e. W, WZ) still to be finalized...

↪ **Will be prepared for a future public release of MATRIX.**

NLO QCD corrections to loop-induced gg channel

- Massless 2-loop amplitudes available [Caola, Henn, Melnikov, Smirnov, Smirnov (2015); von Manteuffel, Tancredi (2015)]
- Squared 1-loop amplitudes available from public tools, e.g. **OPENLOOPS**
- Standard NLO subtraction techniques applicable, e.g. Catani–Seymour dipoles

↪ **Validation within the MATRIX framework is ongoing.**

Sample distributions for gg ($\to W^+W^-$) $\to \mu^+ e^- \nu_\mu \bar{\nu}_e$

[Caola, Melnikov, Röntsch, Tancredi (2015)]

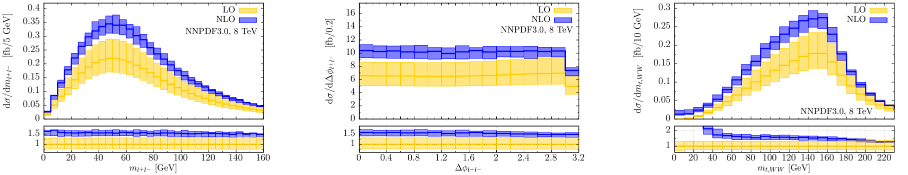

Sample distributions for gg ($\to ZZ$) $\to \mu^+ \mu^- e^+ e^-$

[Caola, Melnikov, Röntsch, Tancredi (2015)]

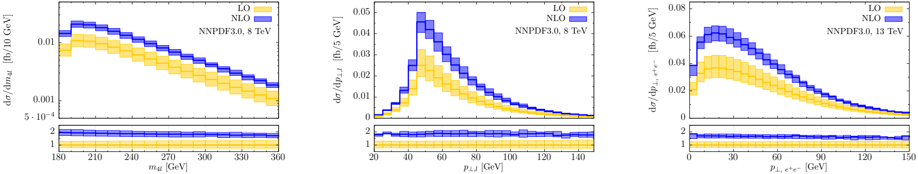

Basic remarks on EW calculations

Dominant effects of NLO EW corrections

- Shape corrections in invariant-mass distributions (if resonances are involved) due to photon bremsstrahlung (depends on photon-recombination procedure)
- Negative corrections in high-energy observables due to Sudakov logarithms

Combination of (N)NLO QCD and NLO EW corrections

- additive: $d\sigma^{\mathrm{(N)NLO}}_{\mathrm{QCD+EW}} = d\sigma^{\mathrm{LO}}(1 + \delta_{\mathrm{QCD}} + \delta_{\mathrm{EW}})$
- multiplicative: $d\sigma^{\mathrm{(N)NLO}}_{\mathrm{QCD\times EW}} = d\sigma^{\mathrm{LO}}(1 + \delta_{\mathrm{QCD}})(1 + \delta_{\mathrm{EW}})$

↪ Multiplicative combination can cover dominant (universal) effects of mixed QCD–EW corrections (uncertainty estimate needed: to which extent?).

Photon-induced processes

- both as LO subprocesses (like $\gamma\gamma \to W^+W^-$) and in NLO EW corrections

↪ They can become sizable in high-energy observables.

NLO EW corrections are implemented in **MUNICH** + **OPENLOOPS** in a fully automated way (and validated in great detail in LH17 proceedings [Andersen et al. (2018)]).

↪ **They will be made available in a future release of MATRIX.**

NLO QCD+EW results for $\mathrm{pp} \to 2\ell 2\nu + \mathrm{X}$ (DF) at 13 TeV

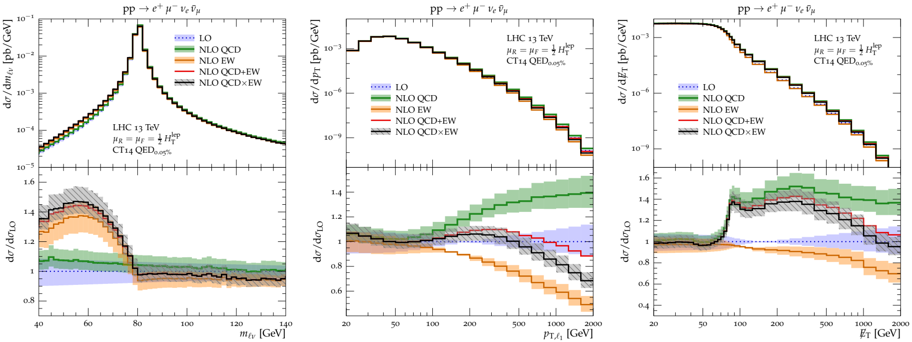

[SK, Lindert, Pozzorini, Schönherr (2017)]

- Distribution in $m_{\ell\nu}$: (left plot) — Shape distortions at NLO EW due to photon bremsstrahlung off the lepton (migration from peak to low-mass tail).
- Distribution in p_{T,ℓ_1}: (central plot) — typical Sudakov suppression in high-p_T tail at **NLO EW**; also **NLO QCD** corrections sizable in tail (moderate jet veto).
  ↪ Considerable mixed **QCD**×**EW** effects expected.
- Distribution in $p_{T,\mathrm{miss}}$: (right plot) — Sudakov effects less pronounced in high-p_T tail.
  ↪ Driven by EW interaction of leptons, not W bosons.

Conclusions

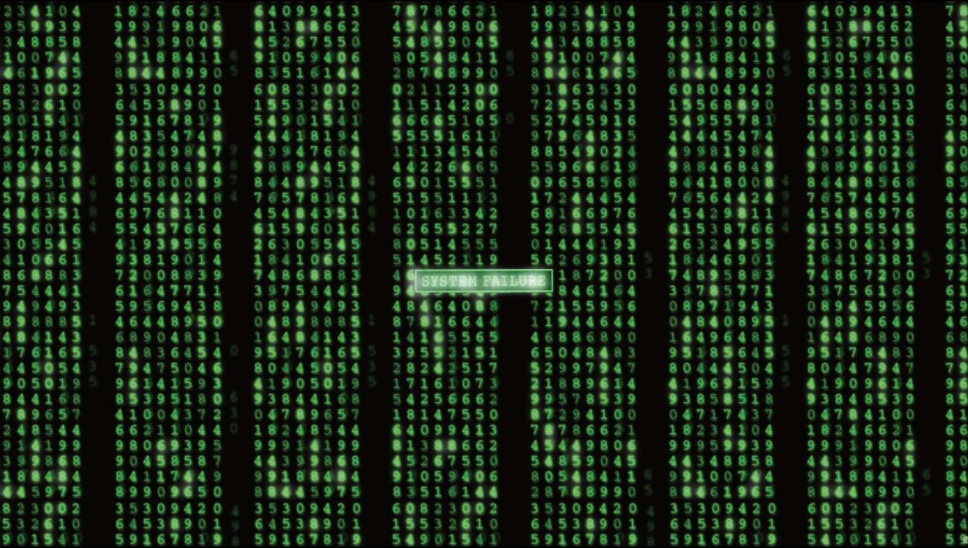

Conclusions

MATRIX – an automated framework to perform fully differential NNLO (+NNLL) QCD computations for colourless final-state production – introduced, which is based on

- the **MUNICH** Monte Carlo integrator,
- the q_{T} subtraction (+resummation) method,
- **OPENLOOPS** and dedicated 2-loop amplitudes from **VVAMP**.

NNLO QCD results calculated in the MATRIX framework

- Fully differential results for $\mathrm{pp}\,(\to \mathrm{V}\gamma) \to \ell\ell\gamma/\ell\nu\gamma/\nu\nu\gamma + \mathrm{X}$
- Inclusive and fully differential cross sections for $\mathbf{pp}\,(\to \mathbf{W^{\pm}Z}) \to \mathbf{3\ell\nu + X}$
  - NNLO/NLO (inclusive): **8%** to **11%** (7 TeV to 14 TeV).
- Inclusive and fully differential cross sections for $\mathbf{pp}\,(\to \mathbf{W^{+}W^{-}}) \to \mathbf{2\ell 2\nu + X}$
  - NNLO/NLO (inclusive): **9%** to **12%** (7 TeV to 14 TeV) (≈ 35% from gg).
  - Different situation with jet-veto: gg dominates, $q\bar{q}$ slightly negative.
- Inclusive and fully differential results for $\mathbf{pp}\,(\to \mathbf{ZZ}) \to \mathbf{4\ell + X}$
  - NNLO/NLO (inclusive): **12%** to **17%** (7 TeV to 14 TeV) (≈ 60% from gg).

↪ Improved agreement between data and theory by NNLO prediction.

First MATRIX release (November 2017)

. . . available for download under https://matrix.hepforge.org .

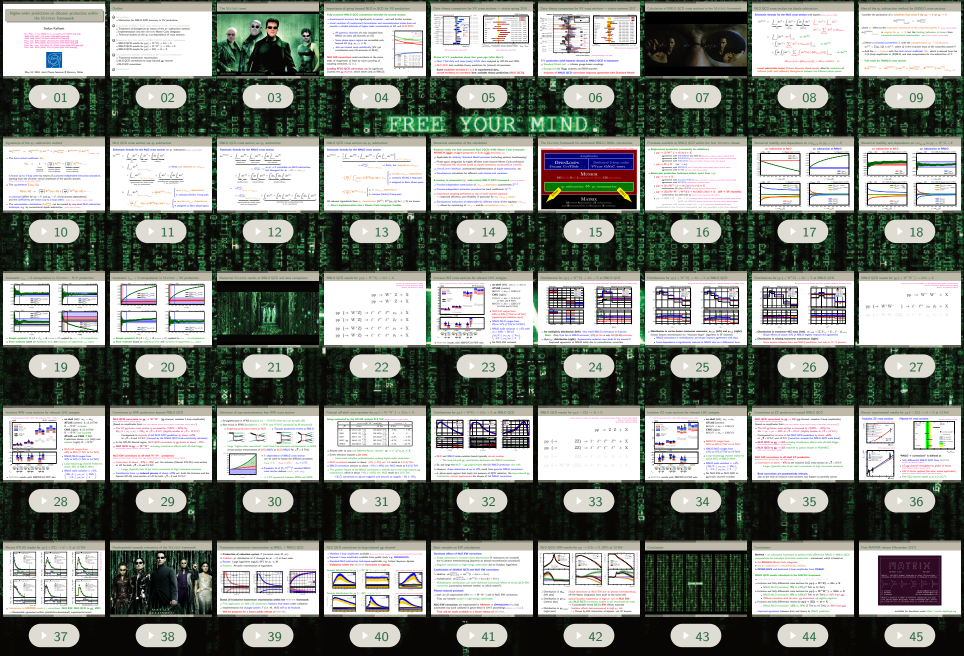
01
02
03
04
05
06
07
08
09
FREE YOUR MIND
10
11
12
13
14
15
16
17
18
19
20
21
22
23
24
25
26
27
28
29
30
31
32
33
34
35
36
37
38
39
40
41
42
43
44
45

Backup


B01
B02
B03
B04
B05
B06
B07
B08
B09
B10
B11
B12
B13
B14
B15
B16
B17
B18
B19
B20
B21
B22
B23
B24
B25
B26
B27
B28
B29
B30
B31
B32
B33
B34
B35

External ingredients: amplitudes applied in the calculation

1-loop amplitudes with OpenLoops [Cascioli, Maierhöfer, Pozzorini (2011); Cascioli, Lindert, Maierhöfer, Pozzorini (2014)]

- All tree and (squared) one-loop amplitudes (including colour/helicity correlations)
- Fully automated compact and fast numerical code for any SM process (QCD+EW)
- **Tensor reduction by means of the Collier library** [Denner, Dittmaier, Hofer (2014)]
  - Numerically stable Denner–Dittmaier reduction methods [Denner, Dittmaier (2002 & 2005)]
  - Scalar integrals with complex masses [Denner, Dittmaier (2010)]
- **Rescue system based on quad-precision CutTools** [Ossola, Papadopoulos, Pittau (2008)]
  - Scalar integrals from OneLOop [van Hameren, Papadopoulos, Pittau (2009); van Hameren (2010)]

2-loop amplitudes from analytic results

- Drell–Yan-like amplitudes from [Matsuura, van der Marck, van Neerven (1989)]
- $V\gamma$ helicity amplitudes from [Gehrmann, Tancredi (2011)] , using TDHPL [Gehrmann, Remiddi (2001)]
- On-shell VV amplitudes from private code [von Manteuffel, Tancredi (2014)] , using GiNaC (applied in [Cascioli et al. (2014); Gehrmann et al. (2014); Grazzini, SK, Rathlev, Wiesemann (2015)])
- Off-shell helicity VV' amplitudes from VVamp [Gehrmann, von Manteuffel, Tancredi (2015)] , using GiNaC [Bauer, Frink, Kreckel (2002); Vollinga, Weinzierl (2005)] (independent calculation by [Caola, Henn, Melnikov, Smirnov, Smirnov (2014)])

Status of VV calculations at NNLO QCD accuracy

- $pp \to \gamma\gamma + X$
  - 2γNNLO (q_T subtraction) [Catani, Cieri, de Florian, Ferrera, Grazzini [arXiv:1110.2375 [hep-ph]]]
  - MCFM (N-jettiness subtraction) [Campbell, K. Ellis , Li, Williams [arXiv:1603.02663 [hep-ph]]]
- $pp \to W(\to \ell\nu)\gamma + X$
  - Matrix (q_T subtraction) [Grazzini, Kallweit, Rathlev [arXiv:1504.01330 [hep-ph]]]
- $pp \to Z(\to 2\ell/2\nu)\gamma + X$
  - Matrix (q_T subtraction)
    [Grazzini, Kallweit, Rathlev, Torre [arXiv:1309.7000 [hep-ph]], Grazzini, Kallweit, Rathlev [arXiv:1504.01330 [hep-ph]]]
  - MCFM (N-jettiness subtraction) [Campbell, Neumann, Williams [arXiv:1708.02925 [hep-ph]]]
- $pp \to WW(\to 2\ell 2\nu) + X$
  - Matrix (q_T subtraction) – on-shell WW and full leptonic decays
    [Gehrmann et al. [arXiv:1408.5243 [hep-ph]], Grazzini, Kallweit, Pozzorini, Rathlev, Wiesemann [arXiv:1605.02716 [hep-ph]]]
- $pp \to ZZ(\to 4\ell) + X$
  - Matrix (q_T subtraction) – on-shell ZZ and full leptonic decays
    [Cascioli et al. [arXiv:1405.2219 [hep-ph]], Grazzini, Kallweit, Rathlev [arXiv:1507.06257 [hep-ph]]]
  - Private implementation (N-jettiness subtraction) – only on-shell ZZ
    [Heinrich, Jahn, Jones, Kerner, Pires [arXiv:1710.06294 [hep-ph]]]
- $pp \to WZ(\to 3\ell\nu) + X$
  - Matrix (q_T subtraction) – on-shell WZ and full leptonic decays
    [Grazzini, Kallweit, Rathlev, Wiesemann [arXiv:1604.08576 [hep-ph], arXiv:1703.09065 [hep-ph]]]

Status of VV calculations beyond NNLO QCD

NNLL+NNLO QCD predictions (transverse-momentum resummation)

- $pp \to \gamma\gamma + X$
  - Private implementation, based on 2γNNLO (q_T resummation) [Cieri, Coradeschi, de Florian [arXiv:1505.03162 [hep-ph]]]
- $pp \to WW/ZZ + X$
  - MATRIX (q_T resummation) [Grazzini, Kallweit, Rathlev, Wiesemann [arXiv:1507.02565 [hep-ph]]]

NLO QCD corrections to loop-induced *gg* channel (leading N³LO contribution)

- $pp \to \gamma\gamma + X$
  - Private implementation [Bern, Dixon, Schmidt [hep-ph/0206194]]
  - MCFM [Campbell, K. Ellis , Li, Williams [arXiv:1603.02663 [hep-ph]]]
- $pp \to WW(\to 2\ell 2\nu) + X$
  - Private implementation [Caola, Melnikov, Röntsch, Tancredi [arXiv:1511.08617 [hep-ph]]]
- $pp \to ZZ(\to 4\ell) + X$
  - Private implementation [Caola, Melnikov, Röntsch, Tancredi [arXiv:1509.06734 [hep-ph]]]

Status of VV calculations at NLO EW accuracy

- $pp \to \gamma\gamma + X$
  - Private implementation (also other on-shell VV processes)
    [Bierweiler, Kasprzik, Kühn [arXiv:1305.5402 [hep-ph]]]
- $pp \to W(\to \ell\nu)\gamma + X$
  - Two independent implementations [Denner, Dittmaier, Hecht, Pasold [arXiv:1412.7421 [hep-ph]]]
- $pp \to Z(\to 2\ell/2\nu)\gamma + X$
  - Two independent implementations [Denner, Dittmaier, Hecht, Pasold [arXiv:1510.08742 [hep-ph]]]
- $pp \to WW(\to 2\ell 2\nu) + X$
  - RECOLA + 2^{nd} independent implementation – only DF channel
    [Biedermann, Billoni, Denner, Dittmaier, Hofer, Jäger, Salfelder [arXiv:1605.03419 [hep-ph]]]
  - SHERPA/MUNICH+OPENLOOPS – SF and DF channels, including $ZZ \to 2\ell 2\nu$
    [Kallweit, Lindert, Pozzorini, Schönherr [arXiv:1705.00598 [hep-ph]]]
- $pp \to ZZ(\to 4\ell) + X$
  - RECOLA + 2^{nd} independent implementation – SF and DF channels
    [Biedermann, Denner, Dittmaier, Hofer, Jäger [arXiv:1601.07787 [hep-ph], arXiv:1611.05338 [hep-ph]]]
- $pp \to WZ(\to 3\ell\nu) + X$
  - RECOLA – SF and DF channels
    [Biedermann, Denner, Hofer [arXiv:1708.06938 [hep-ph]]]

Numerical stability and dependence on $\mathrm{cut}_{q_T/q}$ in $pp \to \gamma\gamma + X$

q_T subtraction at NLO

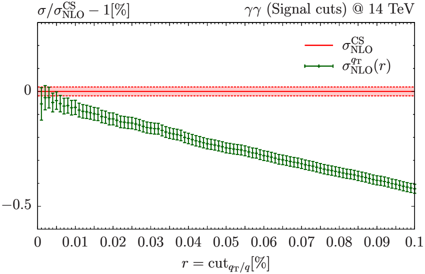

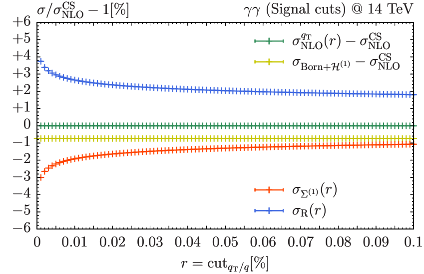

q_T subtraction at NNLO

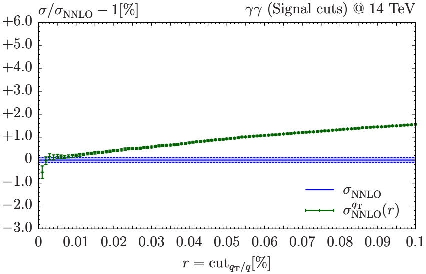

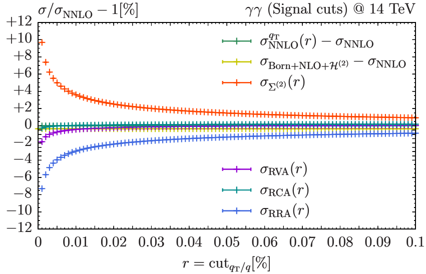

Numerical stability and dependence on $\mathrm{cut}_{q_T/q}$ in $\mathrm{pp} \to \mathrm{W}^+\gamma + X$

q_T subtraction at NLO

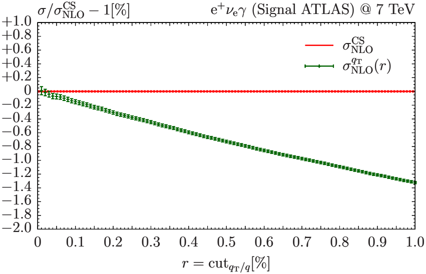

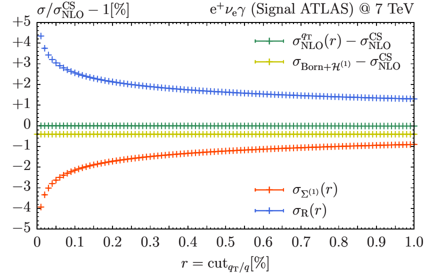

q_T subtraction at NNLO

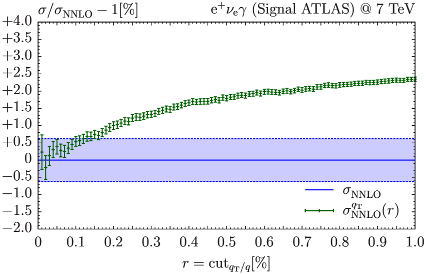

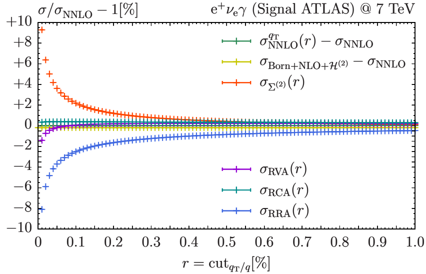

Numerical stability and dependence on $\mathrm{cut}_{q_T/q}$ in $\mathrm{pp} \to \mathrm{W}^+\mathrm{W}^- + X$

q_T subtraction at NLO

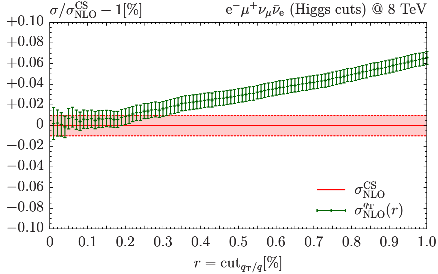

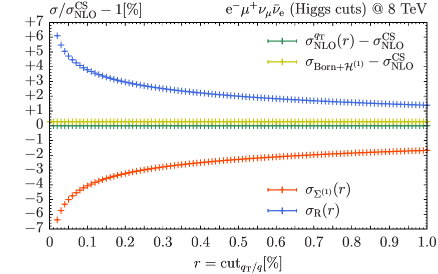

q_T subtraction at NNLO

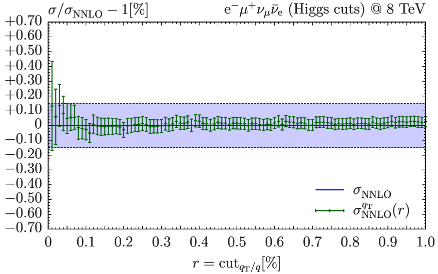

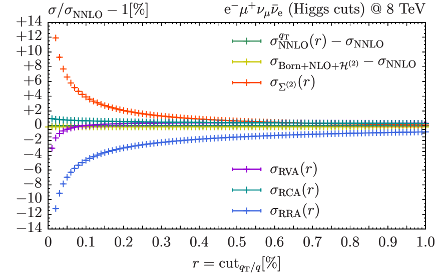

Systematic uncertainties and $\mathrm{cut}_{q_T/q}$ dependence at NNLO QCD

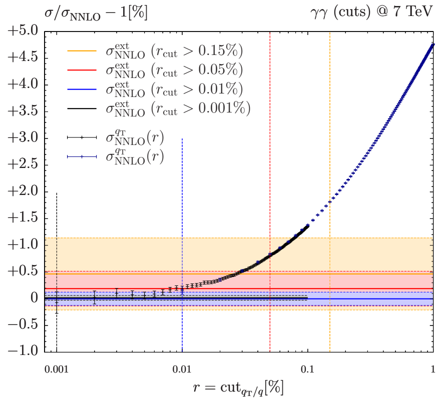

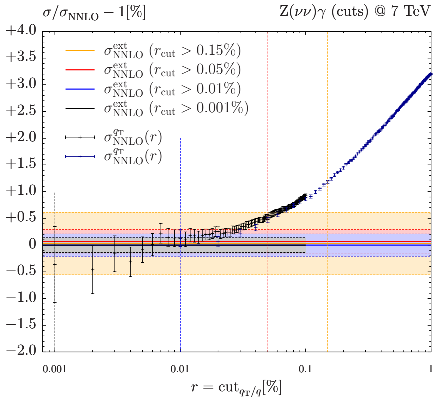

- **Extrapolation $\mathrm{cut}_{q_T/q} \to 0$** by means of empiric ansatz (quadratic fitting curve)
  - Simultaneous evaluation of cross section at various $\mathrm{cut}_{q_T/q}$ values
  - Uncertainty estimate from statistical error and variation of extrapolation range
- **Large cancellation between contributions** $\Rightarrow$ increasing statistical errors
- **No significant $\mathrm{cut}_{q_T/q}$ dependence in VV cross sections (without photons)**

Outlook – Triboson processes at NNLO QCD

Technical checks on feasibility of NNLO QCD calculations to *VVV* production

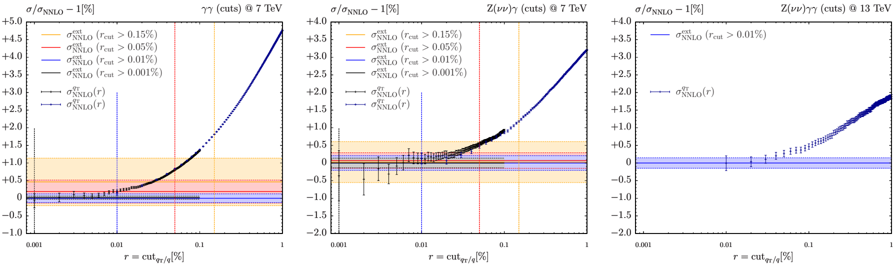

[MATRIX, preliminary]

- Control over cut-off parameter dependence in q_T subtraction is nearly as good for **triboson** (right plot) as for **diboson** (left and central plots) production.
  - ↪ Subtraction already works with present technology within the MATRIX framework (MUNICH [SK] , OPENLOOPS [Pozzorini et al. (2011)] , COLLIER [Denner, Dittmaier, Hofer (2016)]).
- **However:** Two-loop amplitudes for **2** $\to$ **3** processes are not in reach yet.
  - ↪ Amplitudes for $\gamma\gamma\gamma$ or even $V\gamma\gamma$ might become available on timescale of years. . .

NNLO QCD results for $\mathrm{pp}\,(\to \mathrm{V}\gamma) \to \ell\ell\gamma/\nu\nu\gamma/\ell\nu\gamma + \mathrm{X}$

[Grazzini, SK, Rathlev, Torre (2013)]
[Grazzini, SK, Rathlev (2015)]
[Grazzini, SK, Wiesemann (2017)]

$$
\begin{array}{llrllllll}
\mathrm{pp} & (\to & \mathrm{Z}\gamma) & \to & \ell^- & \ell^+ & \gamma & + & \mathrm{X} \\
\mathrm{pp} & (\to & \mathrm{Z}\gamma) & \to & \nu_\ell & \bar{\nu}_\ell & \gamma & + & \mathrm{X} \\
\mathrm{pp} & (\to & \mathrm{W}^+\gamma) & \to & \ell^+ & \nu_\ell & \gamma & + & \mathrm{X} \\
\mathrm{pp} & (\to & \mathrm{W}^-\gamma) & \to & \ell^- & \bar{\nu}_\ell & \gamma & + & \mathrm{X}
\end{array}
$$

Photon isolation

Two contributions to photon production

- Direct production in the hard process,
- Non-perturbative fragmentation of a hard parton.

Different approaches to define isolated photons

- Naive ansatz: forbid any partons inside a fixed cone around the photon.
  ↪ Not infrared safe beyond LO QCD as soft gluons inside the cone are forbidden.
- Hard cone isolation (experimentally preferred)

$$\sum_{\delta'<\delta_0} E_{\mathrm{had,T}}(\delta') \quad \leq \quad \varepsilon_\gamma E_{\gamma,\mathrm{T}}, \qquad\qquad \delta_{i\gamma} = \sqrt{(\eta_i-\eta_\gamma)^2+(\phi_i-\phi_\gamma)^2}$$

  ↪ Only infrared safe if combined with fragmentation contribution (due to quark–photon collinear singularity).
- **Smooth cone isolation** [Frixione (1998)]

$$\sum_{\delta'<\delta} E_{\mathrm{had,T}}(\delta') \quad \leq \quad \varepsilon_\gamma E_{\gamma,\mathrm{T}} \left(\frac{1-\cos(\delta)}{1-\cos(\delta_0)}\right)^n \quad \forall \quad \delta \leq \delta_0$$

  ↪ Smooth cone isolation eliminates fragmentation contribution completely.

Setup for $\mathrm{pp}\,(\to \mathrm{V}\gamma) \to \ell\ell\gamma/\ell\nu\gamma/\nu\nu\gamma + \mathrm{X}$

Setup adapted to the ATLAS analyses @ 7 TeV [ATLAS collaboration (2013)]

	$\mathrm{pp}\,(\to \mathrm{Z}\gamma) \to \ell\ell\gamma + \mathrm{X}$	$\mathrm{pp}\,(\to \mathrm{W}\gamma) \to \ell\nu\gamma + \mathrm{X}$	$\mathrm{pp}\,(\to \mathrm{Z}\gamma) \to \nu\nu\gamma + \mathrm{X}$
Lepton	$p_{\mathrm{T}}^{\ell} > 25\,\mathrm{GeV}$	$p_{\mathrm{T}}^{\ell} > 25\,\mathrm{GeV}$	—
	$\lvert\eta\rvert < 2.47$	$\lvert\eta\rvert < 2.47$	—
Neutrino		$p_{\mathrm{T}}^{\nu} > 35\,\mathrm{GeV}$	$p_{\mathrm{T}}^{\nu\bar{\nu}} > 90\,\mathrm{GeV}$
Photon	$p_{\mathrm{T}}^{\gamma} > 15\,\mathrm{GeV}$ (soft p_{T}^{γ} cut) or $p_{\mathrm{T}}^{\gamma} > 40\,\mathrm{GeV}$ (hard p_{T}^{γ} cut)	$p_{\mathrm{T}}^{\gamma} > 15\,\mathrm{GeV}$ (soft p_{T}^{γ} cut) or $p_{\mathrm{T}}^{\gamma} > 40\,\mathrm{GeV}$ (hard p_{T}^{γ} cut)	$p_{\mathrm{T}}^{\gamma} > 100\,\mathrm{GeV}$
	$\lvert\eta^{\gamma}\rvert < 2.37$	$\lvert\eta^{\gamma}\rvert < 2.37$	$\lvert\eta^{\gamma}\rvert < 2.37$
	Frixione isolation with $\varepsilon_{\gamma} = 0.5$, $R = 0.4$, $n = 1$	**Frixione isolation with $\varepsilon_{\gamma} = 0.5$, $R = 0.4$, $n = 1$**	**Frixione isolation with $\varepsilon_{\gamma} = 0.5$, $R = 0.4$, $n = 1$**
Jets	anti-k_{T} algorithm with $D = 0.4$	anti-k_{T} algorithm with $D = 0.4$	anti-k_{T} algorithm with $D = 0.4$
	$p_{\mathrm{T}}^{\mathrm{jet}} > 30\,\mathrm{GeV}$	$p_{\mathrm{T}}^{\mathrm{jet}} > 30\,\mathrm{GeV}$	$p_{\mathrm{T}}^{\mathrm{jet}} > 30\,\mathrm{GeV}$
	$\lvert\eta^{\mathrm{jet}}\rvert < 4.4$	$\lvert\eta^{\mathrm{jet}}\rvert < 4.4$	$\lvert\eta^{\mathrm{jet}}\rvert < 4.4$
	$N_{\mathrm{jet}} \geq 0$ (inclusive) or $N_{\mathrm{jet}} = 0$ (exclusive)	$N_{\mathrm{jet}} \geq 0$ (inclusive) or $N_{\mathrm{jet}} = 0$ (exclusive)	$N_{\mathrm{jet}} \geq 0$ (inclusive) or $N_{\mathrm{jet}} = 0$ (exclusive)
Separation	$m_{\ell\ell} > 40\,\mathrm{GeV}$	—	—
	$\Delta R(\ell,\gamma) > 0.7$	$\Delta R(\ell,\gamma) > 0.7$	—
	$\Delta R(\ell/\gamma,\mathrm{jet}) > 0.3$	$\Delta R(\ell/\gamma,\mathrm{jet}) > 0.3$	—

Fiducial cross sections for $\mathrm{pp}\,(\to \mathrm{V}\gamma) \to \ell\ell\gamma/\ell\nu\gamma/\nu\nu\gamma + \mathrm{X}$

Setup adapted to the ATLAS analysis @ 7 TeV [ATLAS collaboration (2013)]

process	$p_{\mathrm{T,cut}}^{\gamma}$	N_{jet}	σ_{LO} [pb]	σ_{NLO} [pb]	σ_{NNLO} [pb]	σ_{ATLAS} [pb]	$\frac{\sigma_{\mathrm{NLO}}}{\sigma_{\mathrm{LO}}}$	$\frac{\sigma_{\mathrm{NNLO}}}{\sigma_{\mathrm{NLO}}}$
$\mathbf{Z\gamma} \to \ell\ell\gamma$	soft	≥ 0	$0.8149\,^{+8.0\%}_{-9.3\%}$	$1.222\,^{+4.2\%}_{-5.3\%}$	$1.320\,^{+1.3\%}_{-2.3\%}$	$1.31\ \pm 0.02\ (\mathrm{stat})\ \pm 0.11\ (\mathrm{syst})\ \pm 0.05\ (\mathrm{lumi})$	+50%	+8%
		$= 0$		$1.031\,^{+2.7\%}_{-4.3\%}$	$1.059\,^{+0.7\%}_{-1.4\%}$	$1.05\ \pm 0.02\ (\mathrm{stat})\ \pm 0.10\ (\mathrm{syst})\ \pm 0.04\ (\mathrm{lumi})$	+27%	+3%
	hard	≥ 0	$0.0736\,^{+3.4\%}_{-4.5\%}$	$0.1320\,^{+4.2\%}_{-4.0\%}$	$0.1543\,^{+3.1\%}_{-2.8\%}$		+79%	+17%
$\mathbf{Z\gamma} \to \nu\nu\gamma$		≥ 0	$0.0788\,^{+0.3\%}_{-0.9\%}$	$0.1237\,^{+4.1\%}_{-3.1\%}$	$0.1380\,^{+2.5\%}_{-2.3\%}$	$0.133\ \pm 0.013\ (\mathrm{stat})\ \pm 0.020\ (\mathrm{syst})\ \pm 0.005\ (\mathrm{lumi})$	+57%	+12%
		$= 0$		$0.0881\,^{+1.2\%}_{-1.3\%}$	$0.0866\,^{+1.0\%}_{-0.9\%}$	$0.116\ \pm 0.010\ (\mathrm{stat})\ \pm 0.013\ (\mathrm{syst})\ \pm 0.004\ (\mathrm{lumi})$	+12%	−2%
$\mathbf{W\gamma} \to \ell\nu\gamma$	soft	≥ 0	$0.8726\,^{+6.8\%}_{-8.1\%}$	$2.058\,^{+6.8\%}_{-6.8\%}$	$2.453\,^{+4.1\%}_{-4.1\%}$	$2.77\ \pm 0.03\ (\mathrm{stat})\ \pm 0.33\ (\mathrm{syst})\ \pm 0.14\ (\mathrm{lumi})$	+136%	+19%
		$= 0$		$1.395\,^{+5.2\%}_{-5.8\%}$	$1.493\,^{+1.7\%}_{-2.7\%}$	$1.76\ \pm 0.03\ (\mathrm{stat})\ \pm 0.21\ (\mathrm{syst})\ \pm 0.08\ (\mathrm{lumi})$	+60%	+7%
	hard	≥ 0	$0.1158\,^{+2.6\%}_{-3.7\%}$	$0.3959\,^{+9.0\%}_{-7.3\%}$	$0.4971\,^{+5.3\%}_{-4.7\%}$		+242%	+26%

- Loop-induced gg contributions in $\mathrm{Z}\gamma$ turn out to be very small ($<$ 15% of NNLO).
- Larger K factors in $\mathrm{W}\gamma$ than in $\mathrm{Z}\gamma$ can be explained by breaking of radiation zero.
- Larger K factors in hard than in soft setups due to implicit phase-space restrictions.

Invariant/transverse mass distributions for $\mathrm{pp} \to \ell\ell\gamma/\ell\nu\gamma + \mathrm{X}$

$\mathrm{pp}\ (\to \mathrm{Z}\gamma) \to \ell\ell\gamma + \mathrm{X}$ Distribution in the invariant mass $m_{\ell\ell\gamma}$

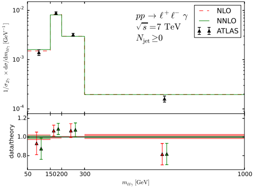

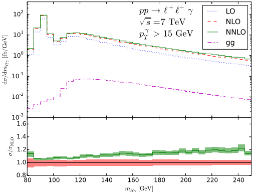

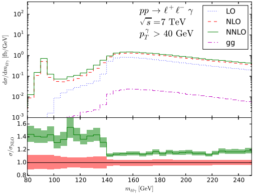

- Implicit LO phase-space restrictions: $m_{\ell\ell\gamma} \approx 66\,\mathrm{GeV}$ (soft) vs. $m_{\ell\ell\gamma} \approx 97\,\mathrm{GeV}$ (hard)

$\mathrm{pp}\ (\to \mathrm{W}\gamma) \to \ell\nu\gamma + \mathrm{X}$ Distribution in the transverse mass $m_\mathrm{T}^{\ell\nu\gamma}$

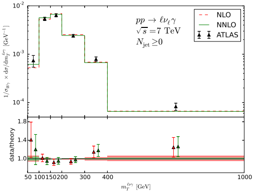

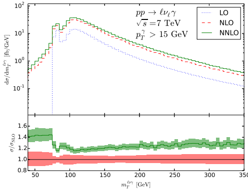

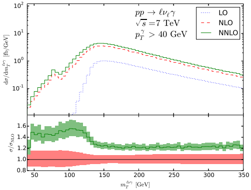

- Implicit LO phase-space restrictions: $m_\mathrm{T}^{\ell\nu\gamma} \approx 75\,\mathrm{GeV}$ (soft) vs. $m_\mathrm{T}^{\ell\nu\gamma} \approx 100\,\mathrm{GeV}$ (hard)

p_{T}^{γ} distributions for $\mathrm{pp}\,(\to \mathrm{Z}\gamma/\mathrm{W}\gamma) \to \ell\ell\gamma/\ell\nu\gamma + \mathrm{X}$

$\mathbf{pp}\ (\to \mathbf{Z}\gamma) \to \ell\ell\gamma + \mathbf{X}$

$N_{\mathrm{jet}} \geq 0$ (left)
$N_{\mathrm{jet}} = 0$ (right)

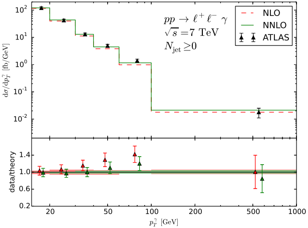

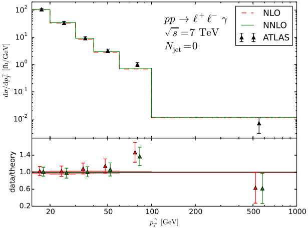

$\mathbf{pp}\ (\to \mathbf{W}\gamma) \to \ell\nu\gamma + \mathbf{X}$

$N_{\mathrm{jet}} \geq 0$ (left)
$N_{\mathrm{jet}} = 0$ (right)

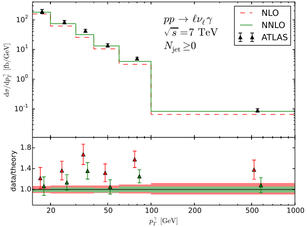

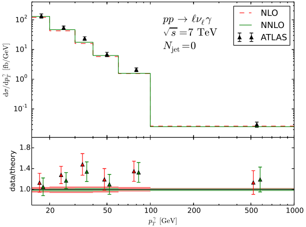

- Agreement between data and theory is significantly improved when including NNLO corrections as compared to NLO prediction, in particular without jet veto.
- No NLO EW corrections included, which become large and negative for higher p_{T}'s.
  [Denner, Dittmaier, Hecht, Pasold (2014 & 2015)]

Comparison between $Z\gamma$ and $W\gamma$ results

Considerably larger K factors in $W\gamma$ than in $Z\gamma$

process	$p_{T,\text{cut}}^{\gamma}$	N_jet	$\frac{\sigma_\text{NLO}}{\sigma_\text{LO}}$	$\frac{\sigma_\text{NNLO}}{\sigma_\text{NLO}}$
$Z\gamma$	soft	$N_\text{jet} \geq 0$	$+50\%$	$+8\%$
$W\gamma$	soft	$N_\text{jet} \geq 0$	$+136\%$	$+19\%$
$Z\gamma$	soft	$N_\text{jet} = 0$	$+27\%$	$+3\%$
$W\gamma$	soft	$N_\text{jet} = 0$	$+60\%$	$+7\%$
$Z\gamma$	hard	$N_\text{jet} \geq 0$	$+79\%$	$+17\%$
$W\gamma$	hard	$N_\text{jet} \geq 0$	$+242\%$	$+26\%$

Explanation: **Breaking of radiation zero beyond LO**

- $u\bar{d}/d\bar{u} \to W^{\pm}\gamma$ amplitudes vanish at $\cos\theta_{q\gamma,\text{CMS}} = \mp 1/3$. [Mikaelian/Samuel/Sahdev (1979)]
- Radiation zero leads to a dip at $\Delta y_{\ell\gamma} = 0$ in pp collisions. [Baur/Errede/Landsberg (1994)]
  - $\hookrightarrow$ Dip filled by higher-order corrections.

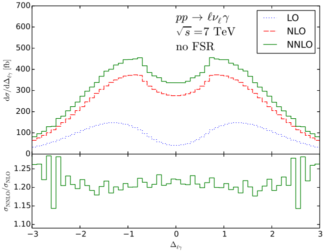

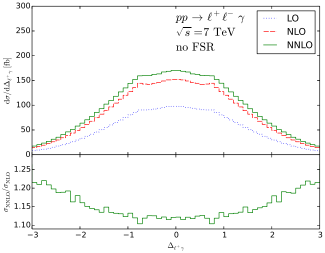

NNLO QCD results for $\mathrm{pp}\,(\to \mathrm{W}^{\pm}\mathrm{Z}) \to 3\ell\nu + \mathrm{X}$

[Grazzini, SK, Rathlev, Wiesemann (2016)]
[Grazzini, SK, Rathlev, Wiesemann (2017)]
[Grazzini, SK, Wiesemann (2017)]

$$\mathrm{pp} \to \mathrm{W}^+ \; \mathrm{Z} + \mathrm{X}$$
$$\mathrm{pp} \to \mathrm{W}^- \; \mathrm{Z} + \mathrm{X}$$

$$\mathrm{pp}\;(\to \mathrm{W}^+\mathrm{Z}) \to \ell^- \; \ell^+ \; \ell'^+ \; \nu_{\ell'} + \mathrm{X}$$
$$\mathrm{pp}\;(\to \mathrm{W}^-\mathrm{Z}) \to \ell^- \; \ell'^- \; \ell^+ \; \bar{\nu}_{\ell'} + \mathrm{X}$$

$$\mathrm{pp}\;(\to \mathrm{W}^+\mathrm{Z}) \to \ell^- \; \ell^+ \; \ell^+ \; \nu_{\ell} + \mathrm{X}$$
$$\mathrm{pp}\;(\to \mathrm{W}^-\mathrm{Z}) \to \ell^- \; \ell^- \; \ell^+ \; \bar{\nu}_{\ell} + \mathrm{X}$$

Distributions for $pp (\to W^{\pm}Z) \to 3\ell\nu + X$ at NNLO QCD

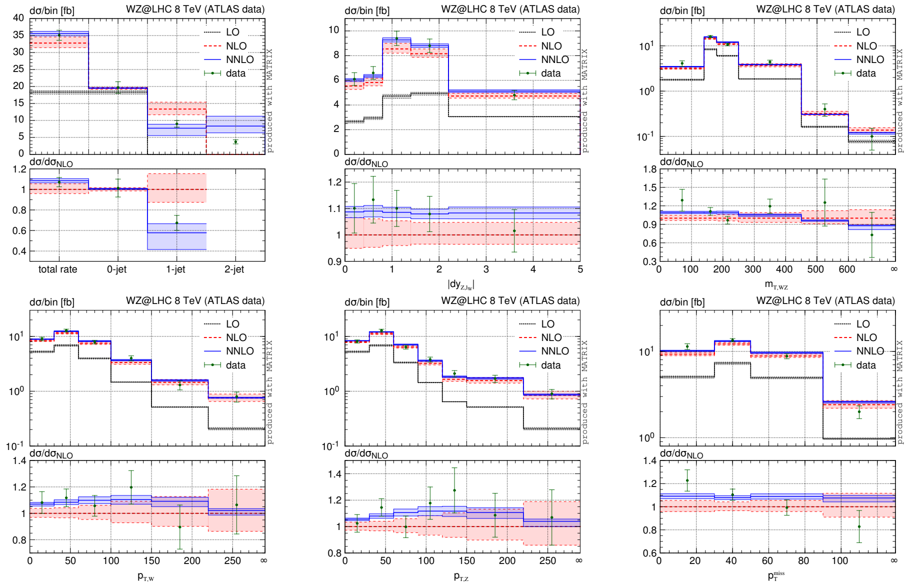

Distributions for $\mathrm{pp}\,(\to \mathrm{W}^{+}\mathrm{Z}) \to 3\ell\nu + \mathrm{X}$ at NNLO QCD

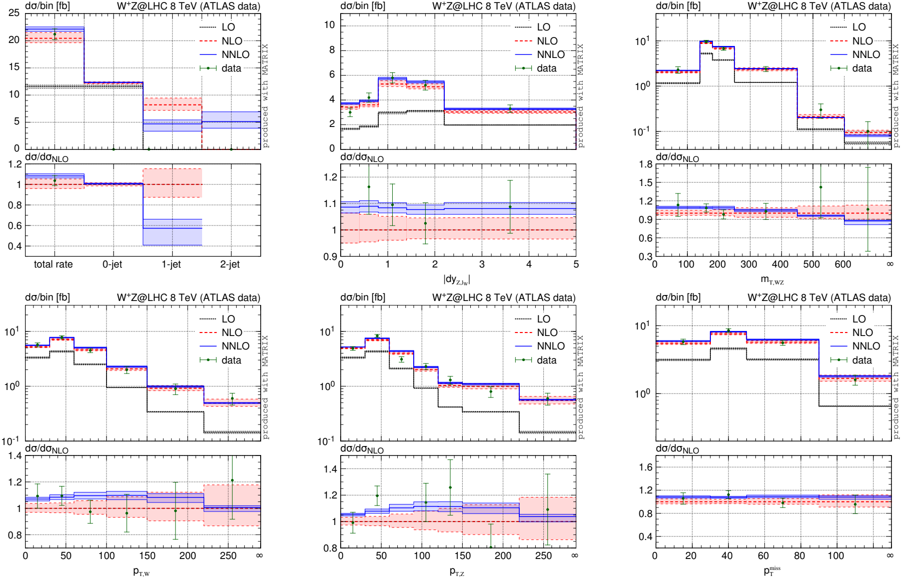

Distributions for $\mathrm{pp}\,(\to \mathrm{W}^{-}\mathrm{Z}) \to 3\ell\nu + \mathrm{X}$ at NNLO QCD

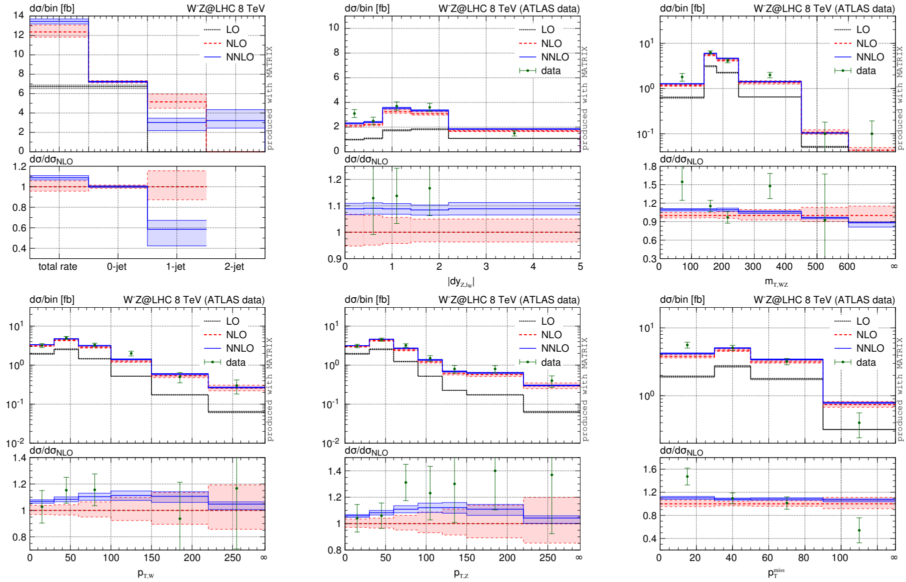

Distribution ratios for $pp\,(\to W^{\pm}Z) \to 3\ell\nu + X$ at NNLO QCD

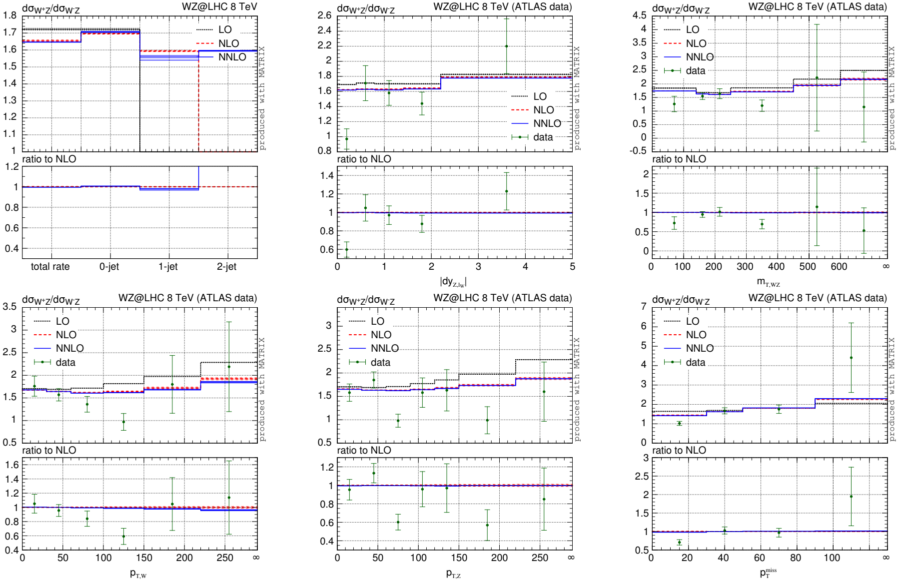

NNLO QCD results for $\mathrm{pp}\,(\to \mathrm{W^+W^-}) \to 2\ell 2\nu + \mathrm{X}$

[Gehrmann, Grazzini, SK, Maierhöfer, von Manteuffel, Pozzorini, Rathlev, Tancredi (2014)]
[Grazzini, SK, Pozzorini, Rathlev, Wiesemann (2016)]
[Grazzini, SK, Wiesemann (2017)]

$$\mathrm{pp} \to \mathrm{W^+} \;\; \mathrm{W^-} + \mathrm{X}$$

$$\mathrm{pp} \;\; (\to \mathrm{W^+W^-}) \to \ell^- \;\; \ell'^+ \;\; \nu_{\ell'} \;\; \bar{\nu}_\ell + \mathrm{X}$$

$$\mathrm{pp} \;\; (\to \mathrm{W^+W^-/ZZ}) \to \ell^- \;\; \ell^+ \;\; \nu_\ell \;\; \bar{\nu}_\ell + \mathrm{X}$$

Definition of top-contamination free WW cross section

- Non-trivial in 5FNS (massless b's $\to$ WW and $\mathrm{WWb\bar{b}}$ connected by IR structure)
  - Single-top production enters at NLO.

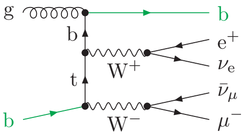

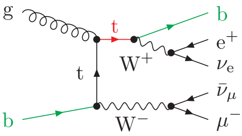

  - Top-pair production enters at NNLO.

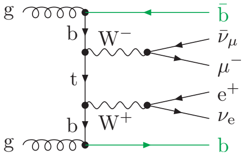

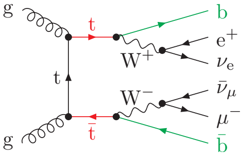

$\hookrightarrow$ Huge "higher-order corrections" result from top-resonance contamination in 5FNS (cross-section enhancement of 30%/400% at NLO/NNLO for $\sqrt{s} = 8$ TeV).

- Straightforward in 4FNS (massive b's $\to$ $\mathrm{WWb\bar{b}}$ finite and can be split off)

Extrapolation in top width to isolate WW contributions

Γ_t-dependence of NNLO cross section can be used to isolate the different processes

- Exploit the Γ_t dependence of the genuine WW, tW, and $t\bar{t}$ contributions,

$$\sigma_{WW} \propto 1, \quad \sigma_{tW} \propto 1/\Gamma_t, \quad \sigma_{t\bar{t}} \propto 1/\Gamma_t^2,$$

  and treat Γ_t as technical parameter to approach the $\Gamma_t \to 0$ limit.

$\hookrightarrow$ Parabolic fit of the $(\Gamma_t/\Gamma_t^{phys})^2$-rescaled cross section delivers σ_{WW}, σ_{tW}, $\sigma_{t\bar{t}}$.

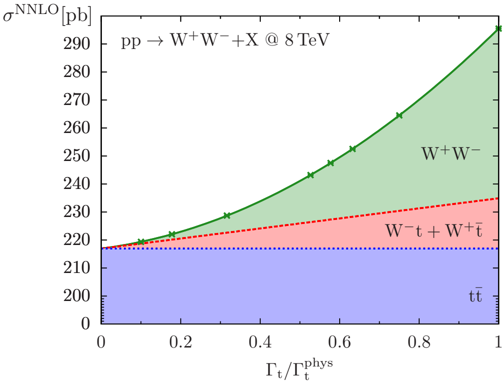

Comparison between 4FNS and 5FNS WW cross sections

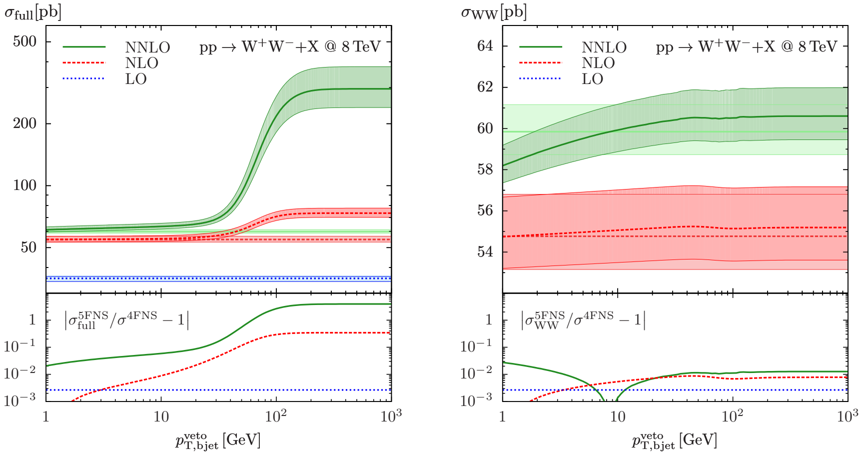

- About 15% of enhancement remain at NNLO for "physical" $p_{\mathrm{T,bjet}}^{\mathrm{veto}} \approx 30\,\mathrm{GeV}$.
- The limit $p_{\mathrm{T,bjet}}^{\mathrm{veto}} \to 0\,\mathrm{GeV}$ cannot be directly accessed (Infrared divergent in 5FNS).
- Extrapolation gives ≈ 1-2% agreement between 4FNS and 5FNS for $p_{\mathrm{T,bjet}}^{\mathrm{veto}} \to \infty$.

Distributions with WW signal cuts: p_{T,l_1}, p_{T,l_2}, $p_{\mathrm{T,miss}}$

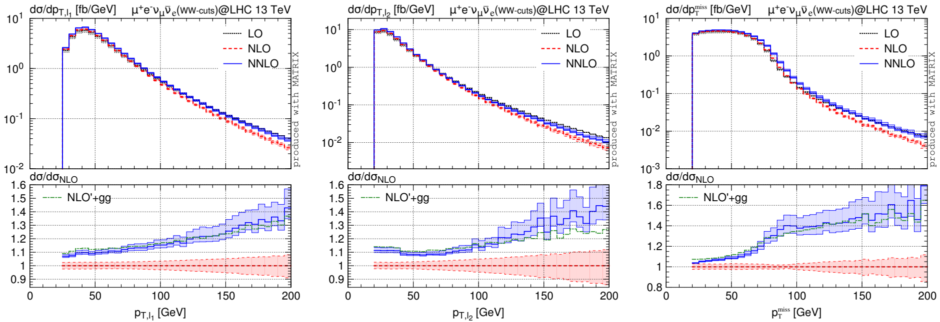

- The loop-induced *gg* contribution dominates the NNLO corrections.
  ↪ NLO and NNLO scale-variation bands typically do not overlap.
  (*gg* channel not covered by scale-variation uncertainties from $q\bar{q}$ channel)
- By and large $\mathrm{NLO}' + gg$ approximates the full NNLO prediction very well (in particular for observables without strong kinematical constraints).
- However, shape distortions of up to about 10% result from genuine NNLO corrections (compared to $\mathrm{NLO}' + gg$ approximation).

Di-lepton distributions with WW signal cuts: m_{ll}, $\Delta\phi_{ll}$, $\Delta\phi_{ll,\nu\nu}$

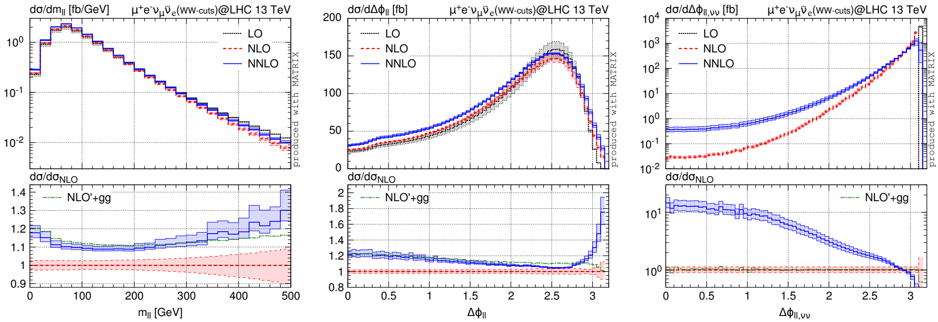

m_{ll} and $\Delta\phi_{ll}$ ($\ll \pi$):

- The loop-induced gg contribution dominates the NNLO corrections.
  - ↪ NLO and NNLO scale-variation bands typically do not overlap.
- Shape distortions of up to about 10% result from genuine NNLO corrections.

$\Delta\phi_{ll}$ ($\lesssim \pi$) and $\Delta\phi_{ll,\nu\nu}$:

- Phase-space regions that imply the presence of QCD radiation:
  - Huge NNLO corrections
  - Loop-induced gg contribution cannot approximate the shapes of full NNLO corrections.

On-shell WW cross section and p_T-veto efficiencies with resummation

Relevant for extrapolation from fiducial to inclusive cross section:

p_T-veto efficiency

$$\epsilon(p_T^{\rm veto}) = \sigma(p_T < p_T^{\rm veto})/\sigma_{\rm tot}\,.$$

The p_T-veto efficiency considered here refers to the transverse momentum of the WW system; it is not the jet-veto efficiency.

However, the two transverse momenta are clearly correlated (and coincide up to $\mathcal{O}(\alpha_s)$).

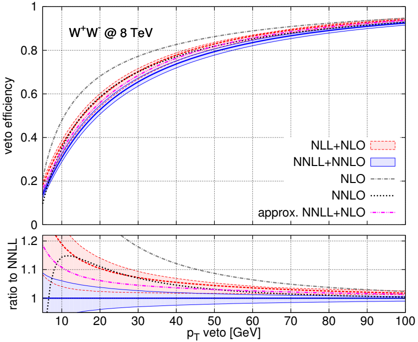

Latest CMS measurement applies approx. NNLL+NLO prediction in the extrapolation:

- CMS WW measurement [CMS collaboration (2015)] : good agreement with NNLO prediction

$$\sigma_{\rm CMS} = 60.1 \pm 0.9({\rm stat}) \pm 3.2({\rm exp}) \pm 3.1({\rm th}) \pm 1.6({\rm lumi})$$
$$\sigma_{\rm NNLO} = 59.84^{+1.3}_{-1.1}({\rm scale}) \pm 1.2({\rm pdf}) \qquad \text{(no Higgs contribution included)}$$

- ATLAS WW measurement [ATLAS collaboration (2016)] : slight excess of $\approx +1.4\sigma$ wrt. NNLO

$$\sigma_{\rm ATLAS} = 71.1 \pm 1.1({\rm stat})^{+5.7}_{-5.0}({\rm syst}) \pm 1.4({\rm lumi})$$
$$\sigma_{\rm NNLO} = 63.2^{+1.6}_{-1.2}({\rm scale}) \pm 1.2({\rm pdf}) \qquad \text{(Higgs contribution included)}$$

NNLO QCD results for $\mathrm{pp}\,(\to \mathrm{ZZ}) \to 4\ell + \mathrm{X}$

[Cascioli, Gehrmann, Grazzini, SK, Maierhöfer, von Manteuffel, Pozzorini, Rathlev, Tancredi, Weihs (2014)]
[Grazzini, SK, Rathlev (2015)]
[Grazzini, SK, Wiesemann (2017)]

$$\mathrm{pp} \to \mathrm{Z}\ \mathrm{Z} + \mathrm{X}$$

$$\mathrm{pp}\ (\to \mathrm{ZZ}) \to \ell^- \ \ell^+ \ \ell'^- \ \ell'^+ + \mathrm{X}$$

$$\mathrm{pp}\ (\to \mathrm{ZZ}) \to \ell^- \ \ell^+ \ \ell^- \ \ell^+ + \mathrm{X}$$

$$\mathrm{pp}\ (\to \mathrm{ZZ}) \to \ell^- \ \ell^+ \ \nu_{\ell'} \ \bar{\nu}_{\ell'} + \mathrm{X}$$

$$\mathrm{pp}\ (\to \mathrm{W^+W^-/ZZ}) \to \ell^- \ \ell^+ \ \nu_{\ell} \ \bar{\nu}_{\ell} + \mathrm{X}$$

Fiducial off-shell cross sections for $\mathrm{pp}\,(\to \mathrm{ZZ}) \to 4\ell + \mathrm{X}$

Setup adapted to the ATLAS analysis @ 8 TeV [ATLAS collaboration (2013)]

channel	σ_{LO} [fb]	σ_{NLO} [fb]	σ_{NNLO} [fb]	σ_{ATLAS} [fb]
$e^+e^-e^+e^-$	$3.547(1)^{+2.9\%}_{-3.9\%}$	$5.047(1)^{+2.8\%}_{-2.3\%}$	$5.79(2)^{+3.4\%}_{-2.6\%}$	$4.6^{+0.8}_{-0.7}(\mathrm{stat})^{+0.4}_{-0.4}(\mathrm{syst})^{+0.1}_{-0.1}(\mathrm{lumi})$
$\mu^+\mu^-\mu^+\mu^-$				$5.0^{+0.6}_{-0.5}(\mathrm{stat})^{+0.2}_{-0.2}(\mathrm{syst})^{+0.2}_{-0.2}(\mathrm{lumi})$
$e^+e^-\mu^+\mu^-$	$6.950(1)^{+2.9\%}_{-3.9\%}$	$9.864(2)^{+2.8\%}_{-2.3\%}$	$11.31(2)^{+3.2\%}_{-2.5\%}$	$11.1^{+1.0}_{-0.9}(\mathrm{stat})^{+0.5}_{-0.5}(\mathrm{syst})^{+0.3}_{-0.3}(\mathrm{lumi})$

- Agreement significantly improved in different-flavour channel.
- Worse agreement in same-flavour channels, but still consistent at the $\approx 1\sigma$ level.

Setup adapted to the ATLAS analysis @ 13 TeV [ATLAS collaboration (2015)]

channel	σ_{LO} [fb]	σ_{NLO} [fb]	σ_{NNLO} [fb]	σ_{ATLAS} [fb]
$e^+e^-e^+e^-$	$5.007(1)^{+4\%}_{-5\%}$	$6.157(1)^{+2\%}_{-2\%}$	$7.14(2)^{+2\%}_{-2\%}$	$8.4^{+2.4}_{-2.0}(\mathrm{stat})^{+0.4}_{-0.2}(\mathrm{syst})^{+0.5}_{-0.3}(\mathrm{lumi})$
$\mu^+\mu^-\mu^+\mu^-$				$6.8^{+1.8}_{-1.5}(\mathrm{stat})^{+0.3}_{-0.3}(\mathrm{syst})^{+0.4}_{-0.3}(\mathrm{lumi})$
$e^+e^-\mu^+\mu^-$	$9.906(1)^{+4\%}_{-5\%}$	$12.171(2)^{+2\%}_{-2\%}$	$14.19(2)^{+2\%}_{-2\%}$	$14.7^{+2.9}_{-2.5}(\mathrm{stat})^{+0.6}_{-0.4}(\mathrm{syst})^{+0.9}_{-0.6}(\mathrm{lumi})$

- Agreement improved at NNLO in all channels within quite large (statistical) errors.

Normalized distributions for off-shell $\mathrm{pp}\,(\to \mathrm{ZZ}) \to 4\ell + \mathrm{X}$

Setup adapted to the CMS analysis @ 8 TeV [CMS collaboration (2015)]

channel	σ_{LO} [fb]	σ_{NLO} [fb]	σ_{NNLO} [fb]
$e^+e^-e^+e^-$	$3.149(1)^{+3.0\%}_{-4.0\%}$	$4.493(1)^{+2.8\%}_{-2.3\%}$	$5.16(1)^{+3.3\%}_{-2.6\%}$
$\mu^+\mu^-\mu^+\mu^-$	$2.973(1)^{+3.1\%}_{-4.1\%}$	$4.255(1)^{+2.8\%}_{-2.3\%}$	$4.90(1)^{+3.4\%}_{-2.6\%}$
$e^+e^-\mu^+\mu^-$	$6.179(1)^{+3.1\%}_{-4.0\%}$	$8.822(1)^{+2.8\%}_{-2.3\%}$	$10.15(2)^{+3.3\%}_{-2.6\%}$

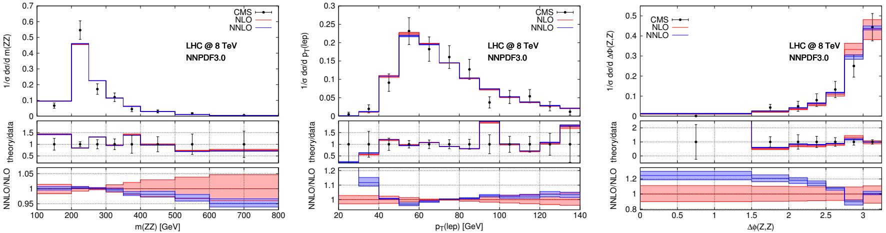

- $m(\mathrm{ZZ})$ and $p_{\mathrm{T}}^{\mathrm{lep}}$ distributions: NNLO effect on shapes dominated by gg contribution, no significant NNLO impact on the data agreement.
- $\Delta\phi(\mathrm{ZZ})$ distribution: Shape agreement improves at NNLO ($\Delta\phi(\mathrm{ZZ}) = \pi$ at LO).

NLO QCD+EW results for $pp \to 2\ell 2\nu + X$ (DF and SF) at 13 TeV

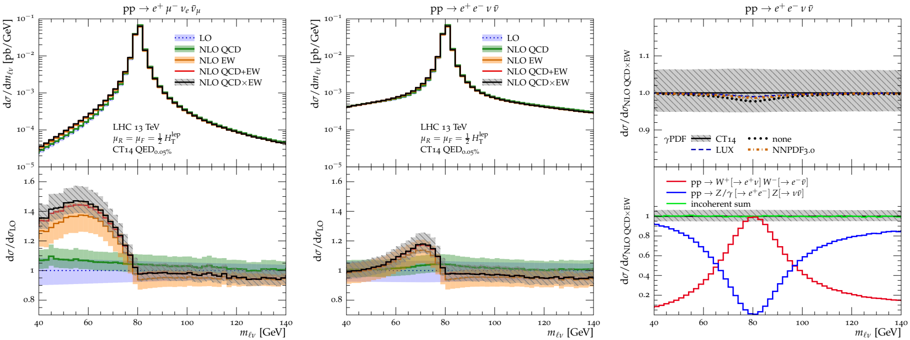

[SK, Lindert, Pozzorini, Schönherr (2017)]

- Different $2\ell 2\nu$ channels involve different resonance structures:
  - **DF channel (left plot):** $pp \to e^+\mu^-\nu_e\bar{\nu}_\mu + X$ (**WW**)
  - **SF channels (central plot):** $pp \to e^+e^-\nu_\mu\bar{\nu}_\mu + X$ (**ZZ**)
    $pp \to e^+e^-\nu_e\bar{\nu}_e + X$ (**WW**/**ZZ**)
- (Pseudo-)observable $\boldsymbol{m_{\ell\nu}}$ undergoes sizable shape distortions at NLO EW due to photon bremsstrahlung off the lepton (migration from peak to low-mass tail).

NLO QCD+EW results for $pp \to 2\ell 2\nu + X$ (DF and SF) at 13 TeV

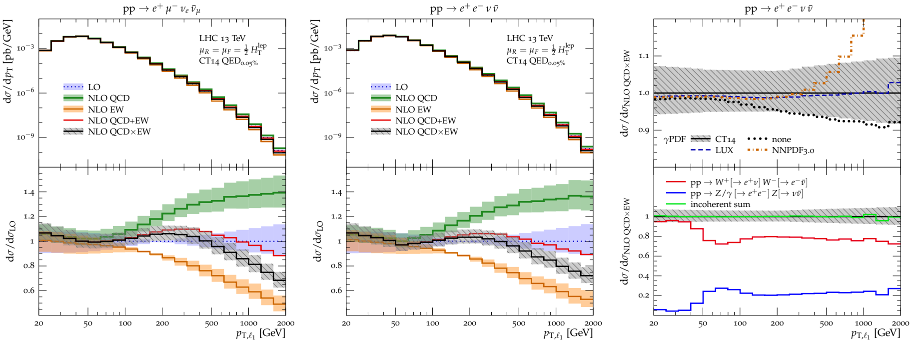

[SK, Lindert, Pozzorini, Schönherr (2017)]

- **DF channel (left plot):** Distribution in p_{T,ℓ_1} exhibits typical Sudakov behaviour in the high-p_T tail ($\approx -40\%$ at 1 TeV).
- **SF channel (central plot):** Separation into *WW* and *ZZ* contributions widely independent of (high) p_{T,ℓ_1}, dominated by *WW*.
  $\hookrightarrow$ Sudakov behaviour in tail (similar to DF case).
- Both **NLO QCD** and **NLO EW** corrections sizable in the tail (moderate jet veto).
  $\hookrightarrow$ Considerable mixed effects expected (approximated by multiplicative combination).

NLO QCD+EW results for $pp \to 2\ell 2\nu + X$ (DF and SF) at 13 TeV

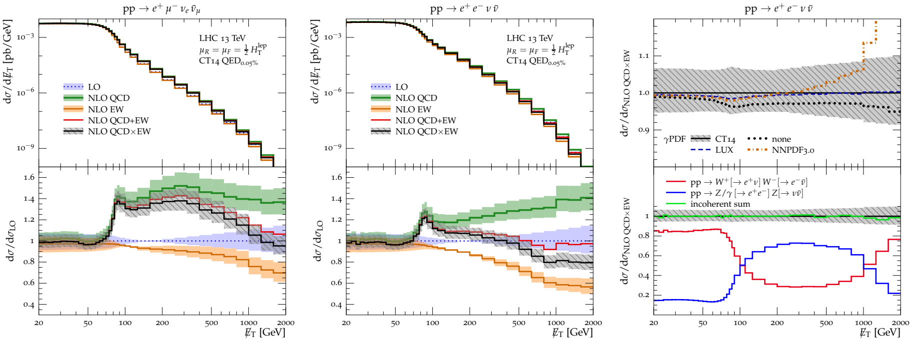

[SK, Lindert, Pozzorini, Schönherr (2017)]

- **DF channel (left plot):** Sudakov effects of distribution in $p_{T,\mathrm{miss}}$ less pronounced (driven by EW interaction of leptons, not W bosons).
  Rather sharp threshold in NLO QCD at $p_{T,\mathrm{miss}} \sim M_W$ (LO subpression of $p_{T,\mathrm{miss}} > M_W$ due to $p_{T,WW} = 0$).
- **SF channel (central plot):** ZZ contributions dominate in intermediate $p_{T,\mathrm{miss}}$ range
  $\hookrightarrow$ typical Sudakov behaviour (driven by Z bosons) up to $p_{T,\mathrm{miss}} \sim 1$ TeV, where WW takes over again.

Conclusions & Outlook

MATRIX – an automated framework to perform fully differential NNLO (+NNLL) QCD computations for colourless final-state production – introduced, which is based on

- the **MUNICH** Monte Carlo integrator,
- the q_T subtraction (+resummation) method,
- **OPENLOOPS** and dedicated 2-loop amplitudes.

Planned extensions of the MATRIX framework:

- Combined analysis of (N)NLO QCD and NLO EW corrections
  - additive or multiplicative combination, uncertainty estimates, etc.
- Implementation of NLO QCD to gg-induced processes (leading N^3LO contribution)
- Reactivation of transverse-momentum resummation
- Extension to q_T subtraction framework with massive quarks in the final state
  - subtraction counterterms implemented and tested [Sargsyan (2017)]
- Extension to N-jettiness subtraction to deal with light jets in the final state
  - performance already proven in V+jet dark-matter background study [Lindert et al. (2017)]
- Application to processes beyond $2 \to 2$, e.g. triple-vector-boson production . . .